UNIVERSIDADE DE SÃO PAULO
INSTITUTO DE FÍSICA DE SÃO CARLOS

NÍCOLAS JUNHITI DE MELO

Natural versus synthetic curcuminoids as photosensitizers: photobleaching and antimicrobial photodynamic therapy evaluation

São Carlos
2022

NÍCOLAS JUNHITI DE MELO

Natural versus synthetic curcuminoids as photosensitizers: photobleaching and antimicrobial photodynamic therapy evaluation

Dissertation presented to the Graduate Program in Physics at the Instituto de Física de São Carlos, Universidade de São Paulo to obtain the degree of Master of Science.

Concentration area: Applied Physics
Option: Biomolecular Physics

Advisor: Dr. Natalia Mayumi Inada
Co-advisor: Dr. Lucas Danilo Dias

Corrected Version

(original version available on the Program Unit)

São Carlos

2022

Melo, Nícolas Junhiti de
Natural versus synthetic curcuminoids as photosensitizers: photobleaching and antimicrobial photodynamic therapy evaluation / Nícolas Junhiti de Melo; advisor Natalia Mayumi Inada; co-advisor Lucas Danilo Dias - corrected version -- São Carlos 2022.
77 p.

Dissertation (Master's degree - Graduate Program in Biomolecular Physics) -- Instituto de Física de São Carlos, Universidade de São Paulo - Brasil , 2022.

1. Photodynamic inactivation. 2. Curcumin. 3. Curcuminoids. 4. Photobleaching. 5. Photochemotherapy. I. Inada, Natalia Mayumi, advisor. II. Dias, Lucas Danilo, co-advisor. III. Title.

À minha família a qual estimo e amo.

ACKNOWLEDGMENTS

Primeiramente à minha família, meu pai Natoniel, minha mãe Adriana e irmã Alícia, com certeza sem eles não conseguiria ser quem eu sou e nem fazer o que eu faço. Mais do que o suporte financeiro nesses tempos difíceis, o apoio emocional e o suporte incondicional nas minhas decisões e na fé que eles têm que eu consigo chegar aonde eu quero, aprecio muito a relação que nós temos e do privilégio que sei que muitos não possuem, nasci numa família muito boa. Também é ótimo ter uma família de cientistas mais ou menos da mesma área para discutir e compartilhar do que cada um faz.

Depois gostaria de agradecer a minha orientadora Natalia pelas carinhosas palavras de motivação e na paciência nos meses em que aparentemente nada funcionava. Não poderia ter pedido melhor orientadora, principalmente nesse período de pandemia que afetou tantos outros grupos e complicou prazos. Também agradeço meu coorientador Lucas pelo apoio e por orientar o projeto enquanto a Natalia teve que se ausentar pela gestação. Aprecio o cuidado em ensinar técnicas e conceitos para minha formação e desejo sucesso nos novos caminhos que irá trilhar.

Aos meus amigos de graduação, Flávia, Cris, Lucas, Lucas (Guincho), Letícia e Angélica por serem incríveis e sempre permitirem que eu desabafasse e compartilhasse de bons momentos e risadas. A pandemia abalou o convívio, mas felizmente sobrevivemos a isso, saibam que a minha decisão de fazer o mestrado em São Carlos é, em partes, por causa de vocês. Tenho receios e ansiedade de não continuar o doutorado aí com vocês, mas ainda bem que hoje em dia podemos nos ver e comunicar pelas salas virtuais do Meet.

Ao grupo de pesquisa, o CEPOF, pela infraestrutura e convívio no mestrado. Dos inúmeros integrantes, gostaria de destacar o Johan, a Jennifer, a Fernanda Alves por terem em todo ou algum momento contribuído com o projeto e que eu pude conhecer um pouco. Ao professor Vanderlei e professora Cristina por contribuírem em reunião para o andamento do projeto e opinar sobre os resultados com seus anos de experiência na área. Certamente não aproveitei o máximo que o grupo tem a oferecer, mas aprecio os bons dias e boas tardes que muitos me deram e por me fazerem pertencer.

Agradeço a Dra. Lívia Dovigo da UNESP – Araraquara pela colaboração na análise estatística dos dados de PDI, o trabalho certamente careceria sem sua ajuda.

Agradeço à USP e ao IFSC pela oportunidade e confiança de participar do programa de pós-graduação e pela infraestrutura dos prédios e salas que frequentei.

Agradeço pela infraestrutura do laboratório fornecida pela Fundação de Amparo à Pesquisa do Estado de São Paulo (FAPESP) (CEPOF 2013/07276-1) e INCT “Basic Optics and Applied to Life Sciences” (FAPESP 2014/50857-8, CNPq 465360/2014-9). Ao Conselho Nacional de Desenvolvimento Científico e Tecnológico (CNPq 132139/2021-9) e Coordenação de Aperfeiçoamento de Pessoal de Nível Superior (CAPES 88887.529586/2020-00 e 88887.601948/2021-00) pelos auxílios da bolsa de estudo.

“Devemos acreditar que somos talentosos para algumas coisas, e que essa coisa, a qualquer custo, deve ser alcançada.”

Marie Curie

ABSTRACT

MELO, N.J. **Natural versus synthetic curcuminoids as photosensitizers:** photobleaching and antimicrobial photodynamic therapy evaluation. 2022. 77p. Dissertation (Master of Science) – São Carlos Institute of Physics, University of São Paulo, São Carlos, 2022.

Curcumin is a well-established photosensitizer in photodynamic therapy due to its natural origin. However, its composition can change based on soil conditions and its extraction generates waste to the environment. As such, a synthetic analogue is preferred since concentration is well set and environmental impact is reduced. However, the differences between natural curcumin and a synthetic analogue as photosensitizers are not well understood and can impact photodynamic inactivation (PDI) reproducibility. Thus, the study on a photophysical level through photobleaching and in PDI was performed. Natural curcumin contains two other curcuminoids, demethoxycurcumin (DMC) and bis-demethoxycurcumin (BDMC), but they are yet to be explored thoroughly in this field and could be as effective or better than the well-known curcumin in, whether individually or mixing all three of them. This thesis seeks to answer these questions and contribute to the curcumin usage in PDI. As such, the photobleaching tests were conducted using spectra from UV-vis spectroscopy and analyzed through numerical solutions to a series of equations of macroscopic photodynamic therapy. The synthetic photosensitizers were tested individually and in six different mixtures, as to investigate how different proportions of naturally found curcumin affect its photodynamic activity. Results obtained show that synthetic curcumin absorbed more of the given light irradiance but generated less singlet oxygen than natural curcumin while also degrading faster than it. However, PDI results showed no significant difference in their inactivation of *S. aureus.* Regarding the other curcuminoids, both DMC and BDMC inactivated up to 5 logs while curcumin inactivated 3.6 logs, this difference raises interest in those molecules. Mixtures of the 3 molecules showed good inactivation results and the best mixtures were those with a medium amount of curcumin and higher content of DMC or BDMC, though they inactivated comparatively to the individual curcuminoids. Therefore, it was observed a synthetic curcumin can replace the natural one and it is a great photosensitizer, DMC and BDMC could be better alternatives that should be further studied in biophotonics.

Keywords: Photodynamic inactivation. Curcumin. Curcuminoids. Photobleaching. Photochemotherapy.

RESUMO

MELO, N.J. **Curcuminoides naturais versus sintéticos como fotossensibilizadores:** avaliação de photobleaching e em terapia fotodinâmica antimicrobiana. 2022. 77p. Dissertação (Mestrado em Ciências) – Instituto de Física de São Carlos, Universidade de São Paulo, São Carlos, 2022.

A curcumina é um fotossensibilizador bem estabelecido no campo da terapia fotodinâmica devido a sua origem natural. Porém, seus componentes podem mudar devido a condições de plantio e sua extração gera lixo ambiental. Dessa forma, um análogo sintético é preferível já que a concentração é definida e o impacto ambiental reduzido. Porém, as diferenças entre curcumina natural e um análogo sintético como fotossensibilizadores não são totalmente entendidas e podem afetar a reprodutibilidade em inativação fotodinâmica (IFD). Assim, foi feito um estudo de suas características fotofísicas através de *photobleaching* e de IFD. A curcumina contém dois curcuminóides, demetoxicurcumina (DMC) e bis-demetoxicurcumina (BDMC), que ainda não foram bem explorados nessa área e sua eficiência pode ser igual ou melhor que a conhecida curcumina, seja em mistura ou isoladamente, na IFD de *Staphylococcus aureus* planctônica. Dessa forma o projeto busca responder essas perguntas não respondidas e contribuir com estudos de curcumina em IFD. Testes de *photobleaching* foram conduzidos analisando espectros de espectroscopia UV-vis e através da solução de uma série de equações da terapia fotodinâmica macroscópica. Os três FSs sintetizados foram testados, individualmente e em 6 misturas diferentes, para investigar como as proporções dos curcuminóides encontrados na curcumina natural podem afetar sua atividade fotodinâmica. Resultados obtidos mostraram que a curcumina sintética absorve mais luz e degradou mais rápido, mas gerou menos oxigênio singleto que a curcumina natural. Porém os resultados de IFD não indicaram diferenças significativas entre os dois em inativar *S. aureus*. Em relação aos outros curcuminóides, tanto DMC quanto BDMC inativaram até 5 logs enquanto a curcumina inativou 3,6 logs, essa diferença cria interesse nessas moléculas. Misturas das três moléculas mostraram bons resultados de inativação e as melhoras misturas foram aquelas com quantidades moderadas de curcumina e maiores de DMC ou BDMC, apesar de inativarem tão bem quanto DMC ou BDMC isoladamente. Portanto, foi observado que a curcumina sintética pode substituir a natural e que curcuminóides DMC e BDMC podem ser alternativas de FS na IFD que devem ser mais estudados na biofotônica.

Palavras-chave: Inativação fotodinâmica. Curcumina. Curcuminoides. Photobleaching. Fotoquimioterapia.

LIST OF FIGURES

LIST OF TABLES

LIST OF ABBREVIATIONS AND ACRONYMS

ATCC	American Type Culture Collection
BDMC	Bis-demethoxycurcumin
BHI	Brain Heart Infusion
CDC	Center for Disease Control and Prevention
CEPOF	Centro de Pesquisas de Ótica e Fotônica
CFU/mL	Colony Forming Unit per milliliter
CUR	Curcumin
DMC	Demethoxycurcumin
DMF	Dimethylformamide
DMSO	Dimethyl Sulfoxide
FDA	Food and Drug Association
FTIR	Fourier Transform Infrared
HPLC	High-performance Liquid Chromatography
IUPAC	International Union of Pure and Applied Chemistry
LPS	Lipopolysaccharide
MRSA	Methicillin-Resistant *Staphylococcus aureus*
PBS	Phosphate-Buffered Saline
PDI	Photodynamic Inactivation
PDT	Photodynamic Therapy
PS	Photosensitizer
ROS	Reactive Oxygen Species
TX-100	Triton X-100
WHO	World Health Organization

SYMBOL LIST

H_2O_2	Hydrogen peroxide
O_2	Molecular oxygen
O_2^-	Superoxide anion
^-OH	Hydroxyl
$^1O_2$	Singlet oxygen
λ	Wavelength
$\tau_{1/2}$	Half-life

SUMMARY

1 INTRODUCTION

1.1 Pathogenic Bacteria: a global health challenge

Pathogenic bacteria have been present throughout human history and associated with mortality and economic loss. The “golden era” of antibiotics in which many new of them were discovered in the 1930s to the 1960s and were used not only in clinical cases but also among armed forces during World War II, saving countless lives. However, as the number of resistant pathogens outpaced the discovery of new antibiotics that era came to an end and the current situation is cause of concern as multidrug-resistant bacteria emerge and could once again prevent conventional treatments, as known medicines would no longer work.[1] Through an economic perspective, antimicrobial resistance represents major financial loss for countries. In the United States only that cost amounts to the billions of dollars for health care and loss of productivity.[2] Furthermore, antimicrobial resistance would impact low-income countries the most as more people will be pushed to extreme poverty and the loss of productivity through sickness and premature death.[3]

As development of antimicrobial techniques become more multidisciplinary, understanding bacteria biology is paramount to researchers who seek to combat said organisms. In a broad sense, bacteria are single-celled and prokaryote organisms and, although for many only pathogenic ones are known, thousands of species are non-pathogenic and are responsible for maintaining life through biogeochemical cycles, such as the nitrogen and carbon cycles, and they help in industrial processes, such as food fermentation and cheese production by *Lactococcus* and *Lactobacillus*.[4]

Metabolic processes occur in the cytoplasm of these microorganisms, where there is a high concentration of solutes in addition to genetic material. To survive osmotic pressure, these cells are delimited by a cell wall, which ensures stiffness and determines their shape. The forms assumed by bacteria can be spheres (coconuts), sticks (bacilli) or spirals (spikes).[5]

In relation to the cell wall, bacteria can be classified mainly into two groups: Gram-positive and Gram-negative bacteria, divided based on the Gram staining test, with the exception of the *genus Mycobacterium* that is not dyed by the Gram technique due to the presence of mycolic acids in the composition of its cell wall. Gram-positive

bacteria have a thick layer of stacked peptidoglycan which allow retainment of the crystal violet stain, while Gram-negative bacteria have a thin layer of peptidoglycan with an outer lipopolysaccharide membrane (LPS), which makes the cell wall more structured. Morphological differences are illustrated in Figure 1.

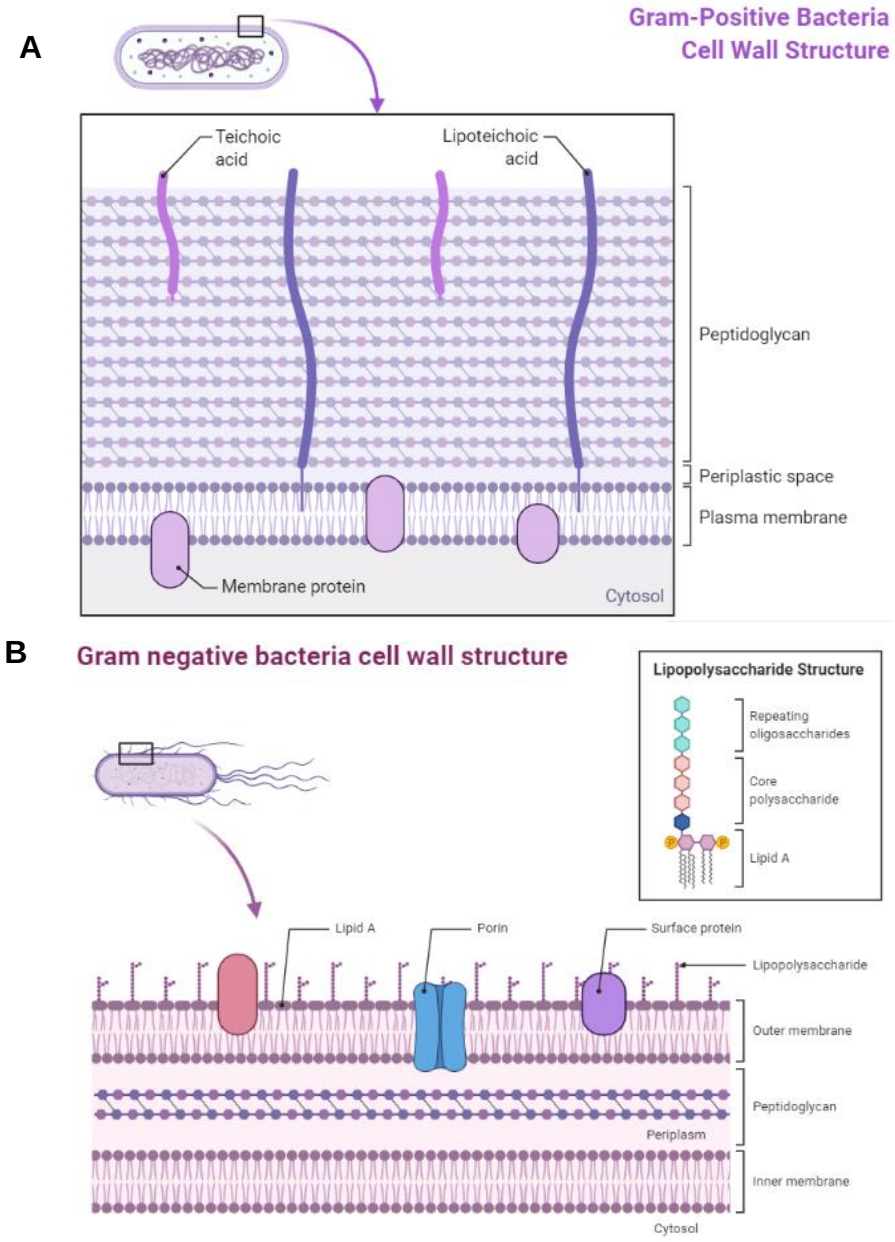

Figure 1 - Cell wall structure of (A)Gram-positive composed of a thick peptidoglycan layer, teichoic and lipoteichoic acids, and a cytoplasmic lipid membrane. (B)Gram-negative bacteria composed of outer and inner membranes enveloping the thin peptidoglycan layer and periplasm, lipid A, and lipopolysaccharides.

Source: Available from: https://app.biorender.com/biorender-templates.

The outer membrane of most Gram-negative bacteria also has a toxic character to animals, due to the presence of lipid A. Some pathogenic bacteria, such *as*

Salmonella and Shigella, are notable for inducing gas formation, diarrhea, and vomiting, and are common in cases of food poisoning.[5]

In addition to the Gram-negative bacteria mentioned above, some Gram-positive bacteria also have pathogenic potential. For example, Gram-positive *Staphylococcus aureus* is responsible for several skin infections, causing reddish spots and blisters to appear and can also become more serious when it enters the bloodstream and infects other regions of the body, such as heart valves and bones, where it causes endocarditis and osteomyelitis, respectively.[6]

The discovery of penicillin by Alexander Fleming in 1928 made it possible for many bacterial diseases to be more easily treatable, but in the years following the discovery, limitations to its use in treatments have been discovered. Socioeconomic changes such as rural exodus and increased population density of cities led to increased exposure of humans to pathogens. The development of new diagnostic tools allowed scientists to more accurately associate bacteria with emerging diseases, and molecular techniques were essential in the differentiation of emerging mutants of *Escherichia coli* and *S. aureus*.[7]

The appearance of resistant bacteria brings new challenges for treatment and is now the cause of thousands of deaths and loss due to hospital infections, bringing additional cost in treatment. According to the Center for Disease Control and Prevention (CDC)'s report published in 2019, about 2,868,700 infections, 35,900 deaths and a billion-dollar financial cost were estimated due to resistant microorganisms in the United States alone. The report also classifies different bacteria into risk classes, warning about possible pathogenic species that may pose serious health risks in a couple of years and the need to develop new therapeutic treatments and antibacterial drugs.[8]

The main mechanisms of action of antibiotics are specific to molecular targets and the modification of these structures by bacterial cells make them ineffective. These changes occur both in the form of spontaneous DNA mutations, as well as by the acquisition of mobile genetic elements of other bacteria or by bacteriophages.[9] In this case, the appearance of resistance can be reported even before the commercialization of new antimicrobials and the uncertainty regarding financial return has caused many pharmaceutical companies to give up investing in the research of new molecules with biological activity different from those already existing in the market. Considering the lack of investments and research in the development of new antimicrobials, there is a

decrease in approvals by agencies such as the Food and Drug Association (FDA); if the current scenario persists, it is estimated that by 2050 we will have 10 million deaths per year due to antimicrobial resistance.[10]

As resistance accumulates faster than the development of new antibiotics, the poor return on research results in less funding from pharmaceutical companies being available. Therefore, research must rely on charity, public funding, and venture capital to seek new innovative approaches to discover new antibiotics that can bypass the various resistances in bacteria, some even reach Phase II. However, the elevated cost of Phase III would have to be financed by big pharmaceutical companies.[11] In the 2020 review by the WHO, only 26 antibiotics were in Phases I – III which target priority targets, of which half target at least one resistant Gram-negative bacteria. Given the high failure rate and possibility of acquired resistance in the development of new antibiotics, the numbers are cause of concern as 19 of those antibiotics in clinical phases are derivates of existing antibiotics and only seven meet the WHO's innovation criteria (absence of known cross-resistance, new target, new mode of action, and/or new class).[12]

Considering all the difficulties regarding the discovery and commercialization of new antibiotics, the research on alternative antimicrobial techniques has propelled, especially Photodynamic Therapy (PDT) as a promising technique whose applications have been growing in recent years.[13]

1.2 Photodynamic Therapy

The use of light to treat skin lesions has been used since the times of ancient civilizations (over 3000 BC). Despite the lack of understanding of the mechanisms of interaction of biological tissue with light, it was used in heliotherapies to maintain good health and in the treatment of other diseases.[14]

In 1903, the Nobel Prize in physics was received by the Danish Niels Finsen for the application of phototherapy in the clinic. In his study, Finsen showed that red light could be used to treat smallpox patients, avoiding suppurations that aggravated the condition of the sick leading to death.[15]

In 1904, then-student at the Pharmacological Institute of Munich Oscar Raab observed that light-sensitive compounds (photosensitive) can be toxic to biological organisms in the presence of light. Raab was working with a *Paramecium caudatum*

culture when he noticed that exposure of white light and acridine caused damage to the microorganism.[16]

Although PDT is already used in skin cancer treatments, its use in microbiological systems has grown more recently, especially after 2014 when the World Health Organization (WHO) warned that we are close to the "post-antibiotic era" due to the appearance of multidrug-resistant bacteria. Thus, *in vitro and in vivo* research has boomed and the mechanisms of action, such as biological targets and associated damage, became better understood.[17]

PDT is a phototherapy that uses photon absorption by a photosensitizing molecule with joint interaction of light and molecular oxygen (O_2) to produce reactive oxygen species (ROS) by two types of reaction. In Type 1 reactions, electron transfer to organic substrates occurs, forming radical ions that interact with O_2 and form hydrogen peroxide (H_2O_2), superoxide radical anion (O_2^-) and hydroxyl (^-OH). In Type 2 reactions (energy transfer) the photosensitizer reacts directly with O_2, exciting it to the singlet oxygen state ($^1O_2$) that interacts with unsaturated lipids, amino acids, proteins and nucleic acids, promoting cell death.[18] The Jablonski diagram (Figure 2) presents the main processes involved in radiation absorption and emission.

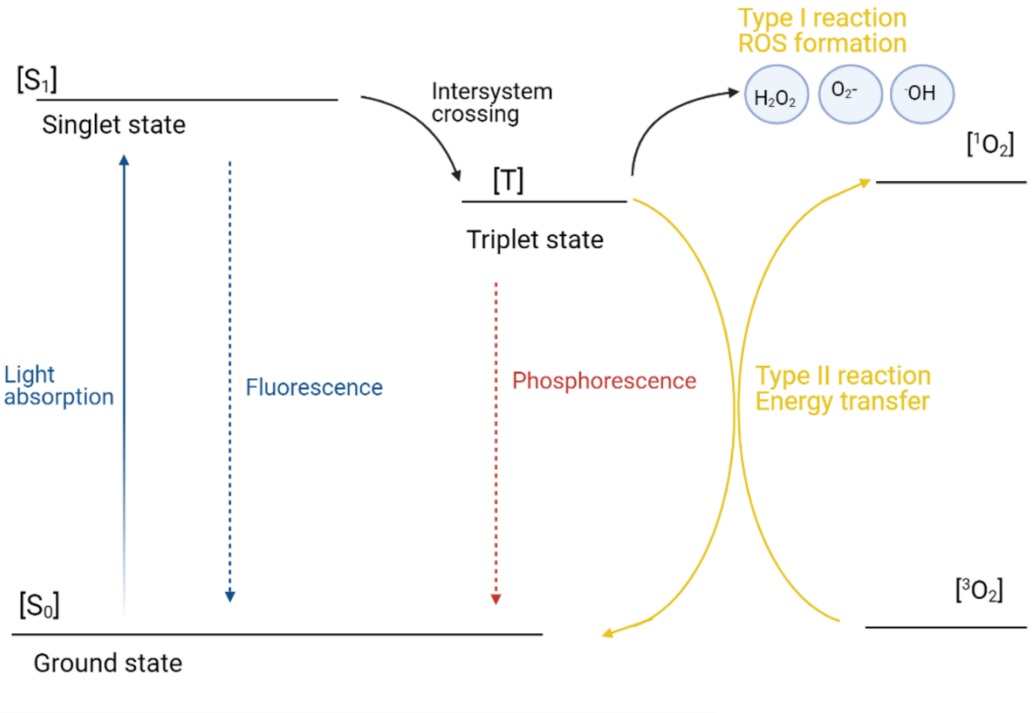

Figure 2 - Simplified Jablonski diagram for PDT illustrating the possible processes an excited photosensitizer can go through such as fluorescence or phosphorescence emission or ROS and $^1O_2$ formation by Type I and II reactions, respectively.

Source: By the author.

Photodynamic inactivation (PDI) is the name given to the use of photodynamic therapy in microbiological systems of interest, such as fungi, bacteria, and viruses. The mechanisms of action for bacterial death described in the literature are related to cell membrane damage, protein inactivation and essential enzymes, and/or DNA damage. Some bacteria have defense mechanisms against oxidative stress and have enzymes that reduce ROS formation, except for singlet oxygen, but the effectiveness of the technique is due to the overload of generated ROS, since the induction of genes responsible for enzyme synthesis activated by ROS takes a few minutes.[19]

The three main parameters considered in PDI experiments are i) the choice of photosensitizer (PS), ii) the light dose emitted and iii) the incubation time or pre-irradiation time. The first step consists of the photosensitizer's capability to enter the bacterial cell or at least adhere to its surface. Cell membrane is negatively charged in both gram-positive and Gram-negative bacteria groups. After this step, the light dose, usually within the visible region (400 – 700 nm), and the most appropriate PS concentration should be established to generate ROS and effectively lead this cell to death.[20]

The choice of PS is the first step in establishing PDT protocols and they can be classified into different classes depending on their molecular structure and origin.[13] The phenothiazin class comprises synthetic dyes, most notably methylene blue and toluidine blue, whose use has already been widely studied in planktonic bacteria, such *as Streptococcus mutans,* and in the partial elimination of biofilms.[21] Tetrapyrrolic macrocyclics are known for their abundance in nature and porphyrins, chlorins and bactereochlorins stand out from this group. Nanostructures also have uses in PDT. Encapsulation of hydrophobic and anionic PSs improves their delivery and photodynamic activity and is an option in the optimization of treatments.[22] The class of natural FSs include molecules of natural origin such as curcumin.

In vitro and in vivo research *on* the efficiency of PDT shows that the technique is capable of inactivating bacteria, fungi, and other microorganisms in a noninvasive and relatively inexpensive manner. Studies carried out in the last 12 years (2010 - 2021) by the Centro de Pesquisas de Ótica e Fotônica (CePOF) are highlighted in Table 1, using curcumin as PS, both natural and synthetic, and illustrate the potential of PDT in planktonic bacteria, biofilms, and in animal models. All studies report at least 2 logs reduction for their respective target organism.

Table 1 - PDI studies in several microbiological systems. The solvent for curcumin is listed in formulation and the state of the microorganism is described in parentheses next to its name.

Entry	Target Organism	Formulation	Concentration	Light dose (J/cm²)	Reference
1	*Trichophyton mentagrophytes* (planktonic)	10% DMSO	6.786 nM 13.57 nM 27.14 nM	2.1 10.52 142	[23]
2	*Candida albicans* (planktonic)	10% DMSO	6.786 nM 13.57 nM 27.14 nM	2,1 10,52 142	[23]
3	*S. aureus* (clinical)	Syrup and candy	2.036 mM	60	[24]
4	MRSA and MSSA (planktonic)	PBS	271 uM	8 and 20	[25]
5	*S. mutans* (planktonic) *S. mutans* (clinical isolate)	Water	203 mM 407 mM 814 mM	24, 48 and 72	[26]
6	*C. albicans* (animal model)	10% DMSO	20 uM 40 uM 80 uM	37.5	[27]
7	*Candida spp.* (planktonic and biofilm)	10% DMSO	5uM 10uM 20 uM 30 uM 40 uM	5.28	[28]
8	*E. coli* and *S. aureus* (in food)	Ethanol	40 uM 80 uM	5, 10 and 15	[29]
9	*Candida albicans* (biofilm)	2% ethanol	4.07 mM	20.1	[30]
10	*Candida albicans* (planktonic)	10% DMSO	0.005 - 20 uM	37.5	[31]
11	*E. coli* (swine skin)	Polyvinylpyrrolidone (PVP)	50 - 100 μM	33.8	[32]

(Continued)

(Continuation)

Table 1 - PDI studies in several microbiological systems. The solvent for curcumin is listed in formulation and the state of the microorganism is described in parentheses next to its name.

Entry	Target Organism	Formulation	Concentration	Light dose (J/cm²)	Reference
12	*Mutans* *L. acidophilus* (biofilm)	Dimethyl D-glucamine	203 mM 407 mM 814 mM 1085 mM 1357 mM	5.7	[33]
13	*Enterococcus faecalis* (biofilm)	10% DMSO	20 uM	30 and 60	[34]
14	*E. coli* (planktonic)	13% DMSO	75 µM	139, 278, 417	[35]
15	*S. pyogenes* *S. mutans(planktonic)*	Syrup (2% w/v)	0.5 - 5 mg/mL	28.8, 60	[36]
16	*S. aureus (animal model)*	1.5% Curcumin gel	0.06 mL of the gel	60	[37]
17	*Streptococcus mutans* *Candida albicans (biofilm)*	Pluronic F-127 micelle	270 µM	15	[38]

Source: By the author.

Despite the proven efficiency of PDI over many microbiological systems, it is verified that there is still room to improve its use. In general, it is observed that Gram-negative bacteria are less susceptible to PDT than Gram-positive bacteria, a fact resulting from the structural differences of their cell walls. Gram-positive bacteria have a cell wall with a thick layer of peptidoglycan, resulting in a more porous cell wall and allows greater diffusion of PS into the cell. On the other hand, Gram-negative bacteria have a thin layer of peptidoglycan, with an external membrane of LPS, which makes the cell wall more structured and more difficult to spread high molecular weight molecules into the cell.[39]

As previously presented, the choice of PS is essential in PDT experiments since the inactivation of the bacteria is dependent on its chemical character. The bacterial cell wall has an anionic character which can affect the ability of cationic FSs to enter the bacteria.

1.3 Natural and synthetic products

The use of natural products as drugs has played a key role in the treatment of diseases for years, specifically for infectious diseases and cancer. These products generally have a complex structure when compared to synthetic molecules and are useful in regulating the endogenous defense of various organisms. Generally in these natural extracts phenols are found, these are secondary metabolites produced by plants to protect themselves against invading organisms. In addition, their historical use can serve as the basis for studies proving efficacy and low toxicity for treatments.[40]

In the area of photodynamic therapy, natural products extracted from plants, such as curcumin and hypericin, are also used, which present photodynamic activity by absorbing visible light. These compounds have curative properties, such as anti-inflammatory, antimicrobial, and even antitumor, and light intensifies its therapeutic potential. Few natural PSs are known, but many studies have been conducted with those discovered.[13]

Despite the advantages presented by natural products for pharmacology and use in photodynamic therapies, determining molecules that have pharmacological activity is an arduous task and often limited by the difficulty of identifying bioactive compounds and the amount of material collected. Environmental conditions in which the natural product is extracted is also an important factor that can alter the present substances, and observed therapeutic effects may not be reproducible, which makes the use of analytical approaches necessary, such as chromatography and spectroscopies, to determine the concentration of metabolites present in a sample.[41]

Another challenge of natural products today is the environmental impact generated by the extraction and subsequent purification of them. Many of the solvents used in the extraction are volatile and potentially toxic, generating waste and toxic co-products that generate environmental pollution.[41]

The difficulties present in this type of approach in the production of new drugs are observed in the decreasing numbers of new drugs based on natural products for antifungal, anticancer and antibacterial treatments in recent years.[42]

In view of the current problem of natural products, the use of synthetic products becomes an attractive option for producing less environmental damage, being easily characterized analytically and by the possibility of large-scale production with defined metabolite concentration. The use of synthetic substances has been growing in recent

years and is an alternative option to the use of natural products, making good use of what is offered by nature and reducing the disadvantages of natural extraction.[42]

1.4 Curcumin

Curcumin is a natural product widely used in Indian cuisine as saffron, being obtained from the rhizomes *of Curcuma longa,* a plant of the Zingiberaceae family. In recent times, the consumption of turmeric has been stimulated due to the numerous therapeutic effects observed and attributed to curcumin and its derivatives. Turmeric is composed of curcuminoid pigments, in addition to some terpenoids (essential oils). A turmeric rhizome may contain 4 to 8 mg/100 g of curcuminoid pigments, and the pigment content may vary according to the age of the root and the region in which it was planted.[43]

Natural curcumin is composed of three curcuminoids (Figure 3), namely curcumin, demethoxycurcumin (DMC) and bisdemethoxycurcumin (BDMC), and extracted from the *C. longa* rhizome. These curcuminoids are used in the Indian medicinal practice *Ayurverda* which makes use of medicinal plants as therapeutic agents, notably for their digestive action, in respiratory diseases and other disorders such as liver diseases. There are also biological records regarding curcumin efficiency due to its anti-inflammatory, antimicrobial, healing and digestive activity.[44]

Curcuminoids are found in *C. longa* rhizome in different proportions: curcumin 77%, DMC 17% and BDMC 3%. However, it is worth mentioning that the curcuminoid content is dependent on planting conditions, which limits, in some cases, the homogeneity of responses of these compounds and makes their synthesis attractive. Depending on planting conditions and plant age, the turmeric rhizome may contain between 2% to 9% curcuminoids.[45]

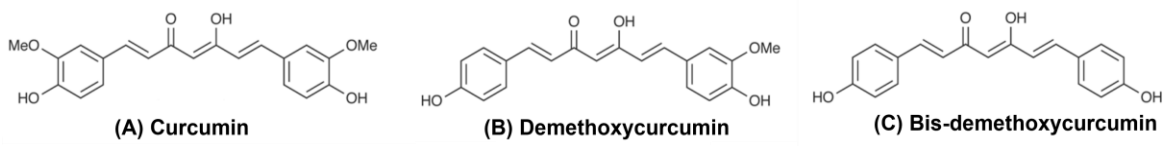

Figure 3 - Chemical structure of the three curcuminoids.

Source: Adapted from Nelson *et al*.[46]

The first curcumin isolation was performed by Vogel in 1815, and its chemical structure was defined by Milobedzka and Lampe in 1910. Characterized as a yellow

crystalline powder of molecular weight 368.39 g.mol^{-1} and chemical formula $C_{21}H_{20}O_6$, the IUPAC nomenclature is (1E, 6E) – 1,7-bis (4-hydroxy – 3-methoxyphenyl) – 1,6-heptadiene-3,5-dione. Curcumin has low solubility in water and ethyl ether but is soluble in ethanol and dimethyl sulfoxide (DMSO). The structure of curcumin is described as a diarileptanoid, having two aromatic groups replaced by methoxy and a phenolic group separated by a polyethylene chain composed of keto-enol group.[45]

The curcumin molecule has keto-enolic tautomerism (Figure 4) and the forms it assumes depend on factors such as temperature, solvent polarity, and aromatic ring replacement.[43] In protic solvents, such as ethanol and DMSO, the enol form is predominant. However, in aqueous solvents, the di-keto form becomes predominant due to the balance of 3 acid-base groups formed with the water molecules, presenting a reddish coloration.[45]

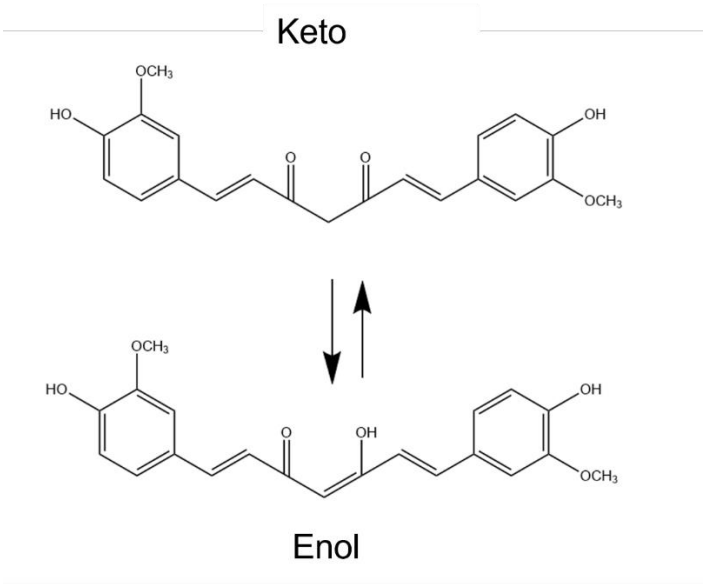

Figure 4 - Keto-enol tautomerism of the curcumin molecule.

Source: By the author.

The first synthesis of curcumin was described by Lampe in 1918 and later refined by Pabon in 1964, reducing the synthesis time while being faster than the process of extraction and isolation of natural curcumin. More recently it was possible to determine the synthesis of DMC and BDMC, bringing advances to the organic synthesis and confirmation of the chemical structure of curcumin, enabling the construction of analogues that potentiate its biological activity and application in PDI.[47] In a study by *Carmona et al*.[48] synthesis of the three curcuminoids was done combining batch and continuous flow setup which allowed curcumin and BDMC to be synthesized

in great amounts per day (24.1 and 20.6 g/day, respectively) while DMC is an extra synthesis step compared to the other two, yielding up to 6.2 g/day.

As described in section 1.3, the use of synthetic molecules is attractive both due to the knowledge of the concentrations of their elements, and the possibility of large-scale production at a low cost. Considering the advances found with curcumin in PDT listed in Table 1, the synthesis of curcumin is of great interest to ensure the reproducibility of protocols in laboratory environments (*in vitro* experiments) and in clinical environments (*in vivo* experiments*)*, where there is interest in optimizing procedures using PDI to ensure effective photodynamic activity in treatment.[49]

1.5 Motivation

PDI is a powerful tool to combat bacteria and other pathological microorganisms and considering the increasing risk of resistant species, in-depth studies on this technique are necessary.

S. aureus is a bacterium of great technical and scientific interest due to the increasing resistance to various classes of antibiotics, *and* methicillin-resistant *S. aureus* (MRSA) is considered a serious threat by the CDC.[10] In addition, because different PS usually follow different parameters for efficient PDI treatment, exploring protocol optimizations with curcumin, DMC, and BDMC will be of great interest to both the research group and the scientific community.

In a study conducted by Silva *et al.* (2017) testing PDI with *Candida albicans* for the treatment of onychomycosis, it was found that curcumin associated with other curcuminoids presented better photodynamic response compared to curcumin alone.[23] Whereas natural curcumin is composed of CUR, DMC and BDMC, this research aims to classify which of the pigments has the highest photodynamic activity against bacteria, as well as to if there is an optimal proportion of the three molecules mixed in solution to improve photoinactivation effects. Thus, in this thesis, the interaction between these molecules was better explored, and experimental parameters such as concentration, light dose and incubation time were established.

In this thesis, the following hypotheses were tested: i. the mixture of curcuminoid pigments has better interaction resulting in greater efficiency of the photodynamic response on inactivation of planktonic *S. aureus*; ii. the concentration of

photosensitizers, incubation time, and doses of light are factors that modulate photodynamic inactivation.

1.6 General Objectives

Evaluate the efficiency of photodynamic therapy (PDT) associated with curcumin, DMC and BDMC, in addition to several combinations of three curcuminoids in the inactivation of a bacterial strains, *S. aureus*.

1.7 Specific Objectives

1. Compare the behavior of natural versus synthetic curcumin by photobleaching experiments through a photodynamic therapy bleaching macroscopic model, and analyze the degradation products formed, oxygen consumption and quantum yield of energetic states;
2. Prepare the combinations of synthetic curcuminoids in the same proportion as the natural extract;
3. Optimize and compare the efficiency of curcuminoids separately and in combination (natural *versus* synthetic) in photodynamic inactivation of *S. aureus (*ATCC 25923);
4. Determine optimal experimental parameters (molar concentration of photosensitizers, incubation time and light dose) in order to better understand differences in the photodynamic efficiency of curcuminoids (natural versus synthetic).

2 NATURAL AND SYNTHETIC CURCUMIN AS PHOTOSENSITIZERS: PHOTOBLEACHING AND ANTIMICROBIAL PHOTODYNAMIC THERAPY EVALUATION

2.1 Context

Aiming to apply curcumin as a photosensitizer, it is possible to obtain a mixture of curcumin and curcuminoids by extracting these pigments from the rhizome of *C. longa* as well as by synthesizing each of the pigments separately in the laboratory in a large scale. In this regard, there are several studies that report the application of curcumin (synthetic and from natural source) indistinctively but there is still a lack of understanding of the efficiency of synthetic curcumin compared to the natural one containing a mixture of photosensitizers such as demethoxycurcumin and bis-demethoxycurcumin.

Synthetic photosensitizers have been used in PDT for some time and curcumin is no exception. Using a synthetic analogue can be beneficial as its contents of curcuminoids is known and it is also less costly, more sustainable, and environmentally friendly. [48, 50]

2.2 Materials and methods

2.2.1 Curcumin preparation

Natural and synthetic curcuminoids were commercially obtained from the PDT Pharma, and/or synthetized by Prof. Kleber de Oliveira´s group.[48] For the preparation of curcuminoid solutions at 4.886 mM, natural or synthetic curcuminoids (18 mg) and DMSO (10 mL) were added and mixed in a test tube. Dilution for later experiments was performed using distilled water to analyze stability via photobleaching and for PDI experiments, the final concentration of DMSO resulted in less than 0.2%.

The stock solutions were kept indoors and at room temperature for a maximum of two weeks to ensure the stability and efficacy of curcumin.

2.2.2 Photobleaching

Firstly, a stock solution of natural and synthetic curcumin from PDT Pharma 4.8 mM was prepared in DMSO, and serial dilutions were performed in distilled water for resulting concentrations of 50 μM, 25 μM and 12.5, and 6.25 μM. Using the Cary UV-Vis50 spectrophotometer, Varian absorption readings from 200 to 800 nm of curcumin solutions were performed in all dilutions. In order to observe photobleaching, the concentration of 50 μM was chosen because it presented high enough absorbance values, which allows to better observe the eventual fall caused by photodegradation. The pH of each solution in distilled water was measured at the pHmeter before the experiment.

The samples were illuminated in a LED-based illumination device, the Biotable®, developed by the Laboratory of Technical Support of the São Carlos Institute of Physics, with average intensity of 40 mW/cm² and the light doses used to observe photobleaching were 5, 10, 20 and 30 J/cm². After each interval the absorption spectrum was collected using the spectrophotometer. Data was processed in Origin to obtain the decay rates resulting from curcumin photodegradation and determination of the best solvent to continue with photodynamic therapy experiments.

2.2.3 Photodynamic therapy bleaching macroscopic model

Given the electronic transitions that appear in the Jablonski diagram for PDT Type I and Type II reactions (Figure 5), a set of differential equations can be deducted, describing the photochemical reactions for every state.[51, 52, 53]

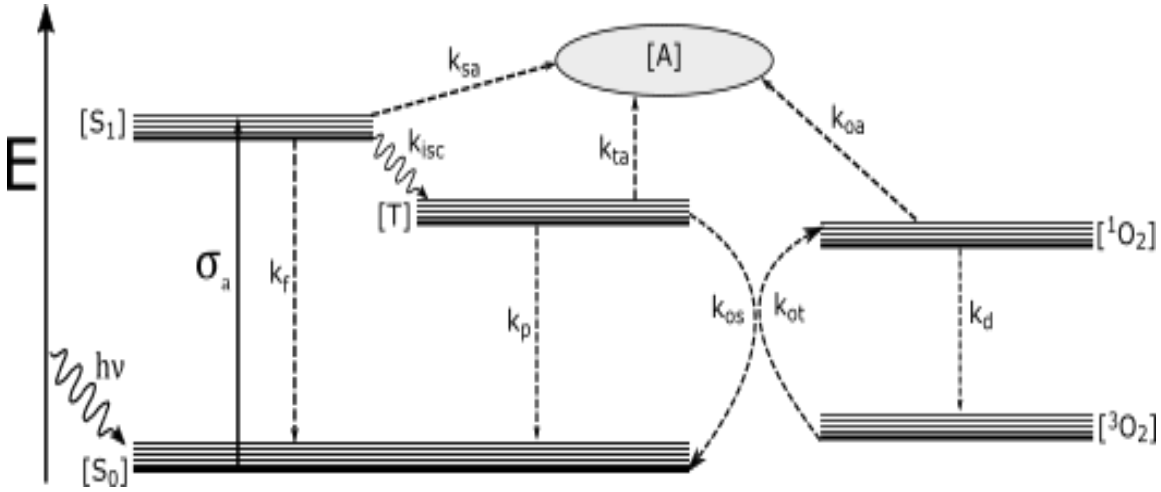

Figure 5 - Jablonski diagram of the main transition found when a photosensitizer absorbs a photon at the correct frequency.

Source: TOVAR *et al.*[54]

$$\frac{d[S_0]}{dt} = -I_a[S_0] + k_f[S_1] + k_p[T] + k_{ot}[T]\left[{}^3O_2\right] - k_{os}[S_0]\left[{}^1O_2\right] \qquad (1)$$

$$\frac{d[S_1]}{dt} = I_a[S_0] - k_f[S_1] - k_{isc}[S_1] - k_{sa}[A][S_0] \qquad (2)$$

$$\frac{d[T]}{dt} = k_{isc}[S_1] - k_p[T] - k_{ot}[T]\left[{}^3O_2\right] - k_{ta}[T][A] \qquad (3)$$

$$\frac{d[{}^3O_2]}{dt} = -S_\Delta k_{ot}[T]\left[{}^3O_2\right] + k_d\left[{}^1O_2\right] + g\left(1 - \frac{\left[{}^3O_2\right]}{\left[{}^3O_2\right]_0}\right) \qquad (4)$$

$$\frac{d[{}^1O_2]}{dt} = S_\Delta k_{ot}[T]\left[{}^3O_2\right] - k_d[{}^1O_2] - k_{oa}[A][{}^1O_2] - k_{os}[S_0][{}^1O_2] \qquad (5)$$

This set of coupled differential equations describes the transitions of the PS when absorbing photons and interacting with surrounding molecules, such as oxygen and it ultimately describes the production of $^1O_2$ which is a major cytotoxic agent produced after PDT.[52]

The terms in brackets refer to each species' concentration and the photochemical constants are listed in Table 2. The equations (1-5) can be written in the quasi-steady state, since the lifetime of the excited species $[S_1]$, $[T]$ and $[{}^1O_2]$ are shorter compared to $[S_0]$, and $\left[{}^1O_2\right]$. Then, the complete set of differential equations can be reduced to two coupled differential equations:

$$\frac{d[S_0]}{dt} = -\frac{C_1}{C_2 + C_3 + C_4[{}^3O_2]}\left(C_2[S_0] + \frac{C_5 C_6[{}^3O_2][S_0]^2}{C_7 + C_6[S_0]}\right) \quad (6)$$

$$\frac{d[{}^3O_2]}{dt} = -\frac{C_1 C_5[{}^3O_2][S_0]}{C_2 + C_3 + C_4[{}^3O_2]}\left(1 - \frac{C_8}{C_7 + C_6[S_0]}\right) + C_9\left(1 - \frac{[{}^3O_2]}{[{}^3O_2]_0}\right) \quad (7)$$

Information on each constant from C_1 to C_9 can also be found below and each variable is described in Table 2. All analyses were performed centering the wavelength absorption at 464 nm.

$$C_1 = \phi_T I_a \qquad C_4 = k_{ot} \qquad C_7 = k_d + k_{oa}[A]$$

$$C_2 = k_{ta}[A] \qquad C_5 = S_\Delta k_{ot} \qquad C_8 = k_d$$

$$C_3 = k_p \qquad C_6 = k_{os} \qquad C_9 = g$$

Table 2 - Definitions and units of variables used in the kinetic analysis.

Symbol	Definition	Units
$[S_0]$	Ground-state sensitizer.	M
$[S_1]$	Excited-state sensitizer.	M
$[T]$	Triplet-state sensitizer.	M
$[{}^3O_2]$	Ground-state triplet oxygen.	M
$[{}^3O_2]_0$	Initial oxygen concentration before PDT treatment.	M
$[{}^1O_2]$	Excited-state singlet oxygen.	M
$[A]$	Cellular targets or acceptor.	M
I_a	Rate of photons absorbed by PS per second ($\frac{\sigma_{so} F_{ex}}{h\nu}$).	s^{-1}
σ_{so}	Absorption cross section of PS.	cm^2
F_{ex}	Irradiance of incident light.	mW cm^{-2}
S_Δ	Fraction of T and $[{}^3O_2]$ reactions that produce $[{}^1O_2]$.	-
ϕ_T	Sensitizer triplet-state quantum yield ($\frac{k_{isc}}{k_{isc}+k_f}$).	-
k_f	Fluorescence constant of $S_1 \rightarrow S_0$	s^{-1}
k_p	Phosphorescence constant of $T \rightarrow S_0$	s^{-1}
k_{isc}	Intersystem crossing of $S_1 \rightarrow T$	s^{-1}
k_d	$^1O_2$ deactivation rate constant	s^{-1}
k_{ot}	BRCQ[a] of T_1 by $^3O_2$	$M^{-1}s^{-1}$
k_{os}	BRCQ[a] of $^1O_2$ by S_0	$M^{-1}s^{-1}$
k_{oa}	BRCQ[a] of $^1O_2$ by A	$M^{-1}s^{-1}$
k_{sa}	BRCQ[a] of S_1 by A	$M^{-1}s^{-1}$
k_{ta}	BRCQ[a] of T_1 by A	$M^{-1}s^{-1}$
g	Maximum oxygen supply rate	Ms^{-1}

[a]BRCQ: Bimolecular rate constant for quenching.

Source: TOVAR *et al.*[54]

2.2.4 Photodynamic Inactivation

The bacterium used for PDI *was S. aureus* (ATCC 25923). To activate the microorganisms, 1 mL of bacteria was inoculated in 9 mL of BHI liquid medium for 16 hours at a temperature of 37° C and a speed of 150 rpm (~0.75g) in a shaker. To work with the bacteria in the mid-log phase, another inoculum was prepared using 1 mL of

the first inoculum and 9 mL of BHI liquid medium, growing under the same shaker conditions for four more hours.

The samples were centrifuged at 15000 rpm for 15 minutes in a bench top centrifuge and resuspended in saline phosphate buffer (PBS) and subsequently diluted to obtain an inoculum with 10^7 - 10^8 CFU/mL, verified by its optical density at 600 nm in the spectrophotometer

The photosensitizer was prepared at 0,5; 1; 5; 10; 25; and 50 µM, mixing 200 µL of curcumin and 200 µL of bacteria, and incubating them for 20 minutes at 37° C. In a 24 well plate, irradiations were performed in the 450 nm Biotable® device, whose intensity is 40 mW/cm², illuminating the samples for 4 min 10 s, 8 min 20 s, and 12 min 30 s, thus delivering fluencies at 10, 20, and 30 J/cm² respectively.

In each experiment, samples were collected for the control groups (bacteria + PBS), light control (bacteria + PBS + light), PS control (bacteria + PBS + PS) and PDI group (bacteria + PBS + PS + irradiation). Subsequently, all groups were submitted to serial dilutions and cultured in Petri dishes containing BHI agar medium for 24 hours to perform colony counting and determination of colony-forming units per milliliter (CFU/mL) (Figure 6).

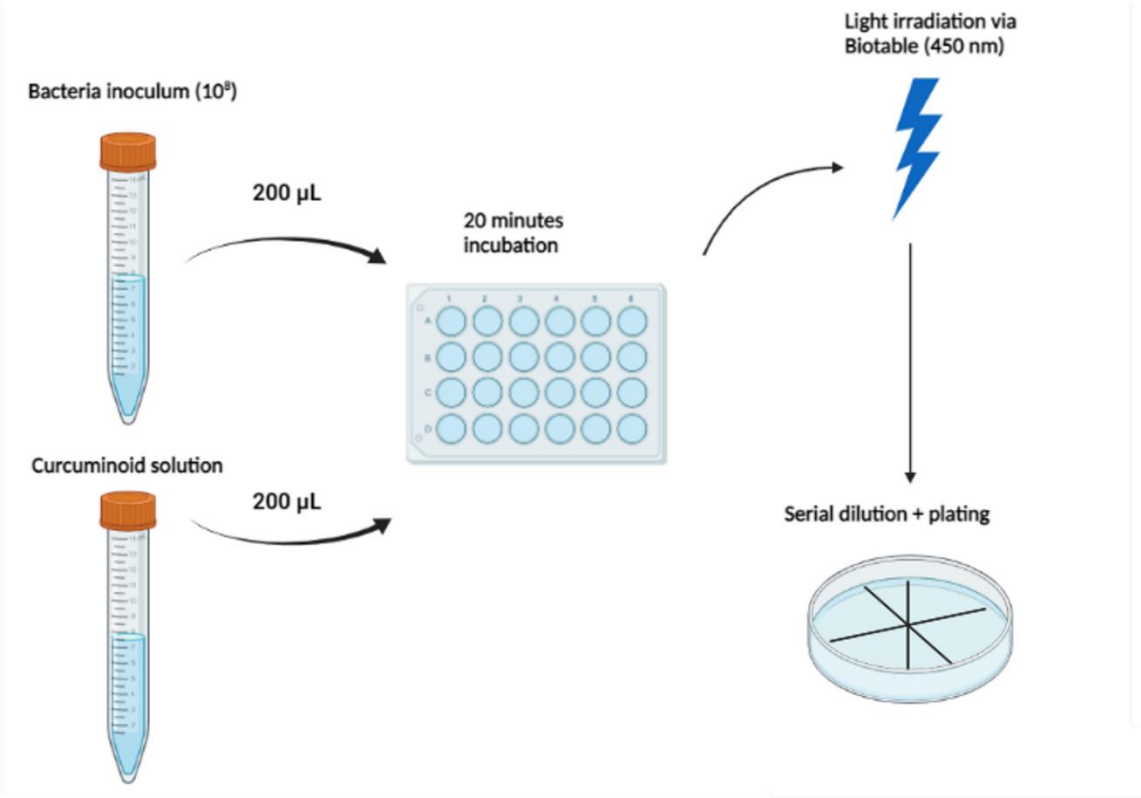

Figure 6 - Methodology for a PDI experiment.

Source: By the author.

2.2.5 Statistical analysis

Each group was tested in triplicate in three different occasions (n=9). After performing descriptive analysis and checking assumptions of normality and homoscedasticity, a two-way analysis of variance was performed, followed by Games-Howell post-hoc test. The two independent factors considered were type of curcumin (natural vs synthetic) and treatment groups and significance level was set at 0.05.

2.3 Results and discussion

2.3.1 Photobleaching

Photobleaching is an experiment that can be used to track down how irradiation degrades the photosensitizer, and it can lead to interesting findings such as the quantum yield of energetic states, how much oxygen is consumed, production of singlet oxygen, and what is the leftover concentration of curcumin after light irradiation.[52]

The absorption curves for both curcumins used and their photobleaching pattern were assessed using the spectrophotometer and spectra are shown in Figure 7. Spectra shown are the mean result of 3 measurements made in different days.

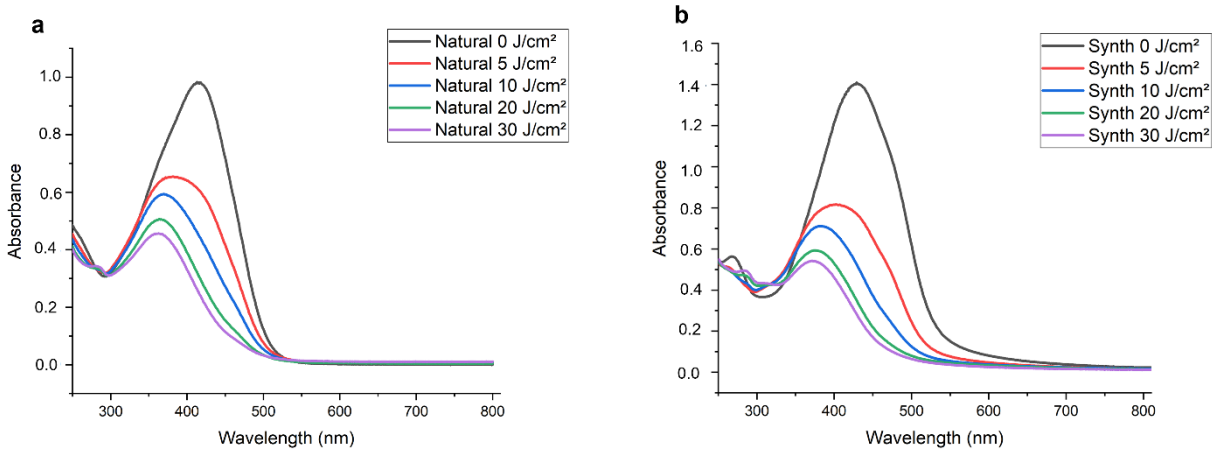

Figure 7 - Photobleaching pattern for both curcumins used at a concentration of 50 μM. a. Natural curcumin b. Synthetic curcumin.

Source: By the author.

Considering the spectra obtained, qualitatively, both had a similar peak in the 410 – 430 nm region and upon irradiation they blue-shifted and their absorbance slightly decreased, possibly indicating aggregation and photodegradation. A more thorough investigation on the PDT reaction that is most prominent and possible degradation pathways is possible using the macroscopic model for PDT bleaching mentioned in section 2.2.5.

2.3.2 Analytical analysis

The Beer-Lambert law relates the absorption of light (A) at a certain wavelength passing through an optical path (L) to the solute concentration (C) and considering the molar attenuation coefficient of the solute (ε).

$$A(C) = \varepsilon . L . C \qquad (8)$$

This law has some limitations in its practical use, most notably high concentrations of the solute tend to break the linear relationship between absorption and concentration. In order to determine the molar attenuation coefficient, readings of absorbance using different concentrations of curcumin were measured at 464 nm. This wavelength was chosen since it coincided with the Biotable's wavelength where irradiance is at its maximum. According to the Beer-Lambert law, a linear plot (Figure 8) can be used to estimate the value of ε for this specific wavelength.

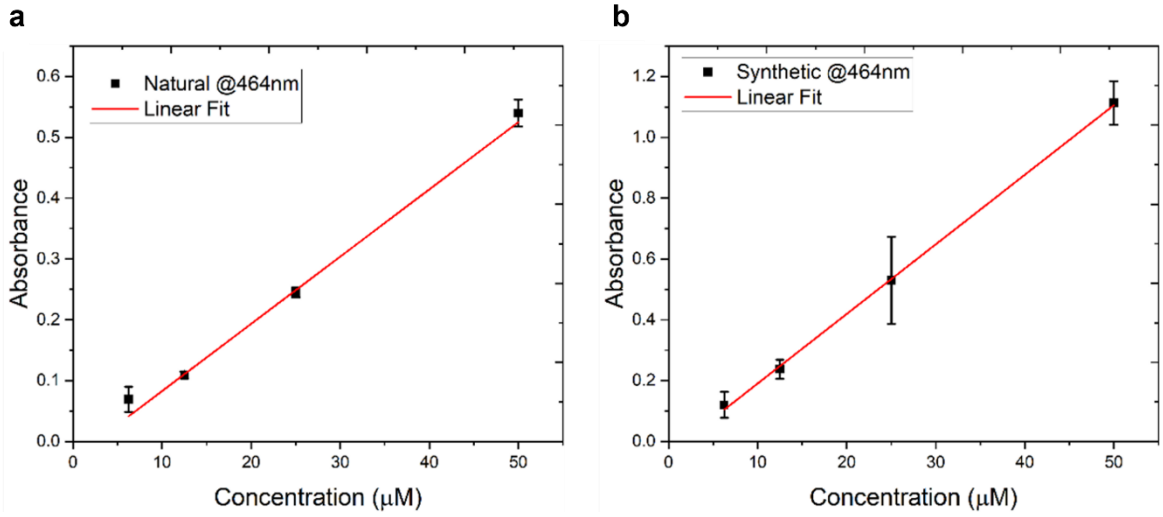

Figure 8 - Plotting of the absorbance value at 464 nm against the solute concentration for a. natural curcumin b. synthetic curcumin.

Source: By the author.

The linear fit obtained for this experimental data had a slope of 0.011 (R^2 of 0.992) for natural curcumin, and 0.023 (R^2 of 0.997) for synthetic curcumin. The molar attenuation coefficients calculated for these curcuminoids were $\varepsilon_{Nat}(464nm) = 1.1x10^4 M^{-1}cm^{-1}$ and $\varepsilon_{Synth}(464nm) = 2.3x10^4 M^{-1}cm^{-1}$.

Another important constant can be calculated with ε is the molecular absorption cross-section in the specified wavelength (σ(λ)) given the relation:

$$\sigma(\lambda) = \frac{2.303\ \varepsilon(\lambda)}{N_A} \qquad (9)$$

N_A being the Avogadro number. Thus, the values obtained for both curcumins were: $\sigma_{Nat}(464nm) = 4.2x10^{-17}cm^2$ and $\sigma_{Synth}(464nm) = 8.7x10^{-17}cm^2$.

With these newfound parameters, we could monitor the curcumin solution's concentration over the photobleaching experiment. To find the numerical solutions to equations (6-7), a code developed in MATLAB by a fellow PhD student in our group was used, solving the model using *ode15* which is a tool to solve differential equations. The initial conditions for curcumin concentration ($[S_0]$) and dissolved oxygen in the sample ($[\ ^3O_2]$) were provided, and for constants C_1 to C_8 guesses were made (Table 3), taking into consideration articles that explored said parameters for curcumin in different solvents. In order to find the best fit for the experimental data, the least-squares method was used, and upper and lower bounds for C_1 to C_8 were taken into consideration as well. C_9 was measured initially through an oximeter and it was the maximum value for g before photobleaching assays.

Table 3: Input guesses for constants C_1 to C_9 for natural and synthetic curcumin and the best fit for each of them considering lower and upper bounds.

Constant	Initial guess	Lower bound	Upper bound	Best fit (natural curcumin)	Best fit (synthetic curcumin)
C_1	1.00E-01	1.00E-02	1.00E+01	0.18456	0.12243
C_2	1.00E+04	1.00E+03	1.00E+05	1.05E+03	1.03E+03
C_3	1.00E+03	1.00E+02	1.00E+04	2077.77013	7323.85984
C_4	1.00E+02	1.00E+02	1.00E+04	3.19E+03	1.79E+03
C_5	1.00E+00	1.00E+01	1.00E+03	9.99E+02	1.00E+03
C_6	1.00E+04	1.00E-01	1.00E+01	9.70E+00	9.98E+00
C_7	1.00E+03	1.00E+03	1.00E+05	5.67E+03	5.51E+03
C_8	1.00E+03	1.00E+02	1.00E+04	1.75E+03	4.55E+02
C_9	5.00E-01	0.00	1.00E+00	0.99893	0.99862

Source: By the author

In Figure 9, the experimental values of curcumin concentration during the photobleaching experiment are shown accompanied by the best fit of $[S_0]$ (t). In Table 4, the constants obtained using the bleaching macroscopic model for curcumin and synthetic curcumin are presented. The dissolved oxygen concentration was also obtained as it is shown in Figure 9.

Figure 9 presents the nonlinear decay of both curcumin and the oxygen consumption during the illumination. As can be observed in Figure 9a, the synthetic curcumin seems to have had a faster decay than natural curcumin with $\tau_{1/2}$ of 135.2 s and 173.0 s respectively. Also, in Figure 9b, even when the samples were in an air-saturated environment (that is, all measurements were made with an open cuvette with optical path 1 cm) a faster oxygen consumption was observed for synthetic curcumin than natural curcumin. After that consumption, a local minimum can be observed at 165.4 s and 248.7 s for synthetic and natural curcumin respectively. Also, a recovery in the oxygen concentration was observed for both curcumins, indicating that, probably, there were no more curcumin/oxygen interactions. Chignell *et al*.[55] observed that 35% of the oxygen initially present in a SDS micellar solution in D_2O of curcumin were consumed, and subsequent recovery indicated possible production, albeit small, of hydrogen peroxide (H_2O_2). Using the constants obtained by the model, we estimated

the value of the ϕ_T in H_2O as 0.047 and 0.015 for natural and synthetic curcumin, respectively. These values are one order of magnitude lower (0.11 ± 0.03) than the one reported by Gorman *et al*.[56] for curcumin in benzene. However, Khopde *et al*.[57] reported value of ϕ_T of our order of magnitude in methanol, DMF, DMSO, TX-100 of 0.03, 0.06, 0.05, and 0.07 respectively. The quantum yield of singlet oxygen, ϕ_Δ, can also be estimated from the fitted values of the experiments. The values obtained were 0.015 and 0.008 for natural and synthetic curcumin, respectively. These values are very low compared with other photosensitizers found in the literature (Protoporphyrin: 0.60, chlorin e_6: 0.75, methylene blue: 0.49)[58], indicating that curcumin, in fact, does not act preferentially via a type 2 reaction. Chignell *et al*.[55] reported the ϕ_Δ for curcumin in different solvents, finding values of 11% in solvents like toluene, benzene, and acetonitrile, however, in solvents like ethanol, iso-propanol, SDS, and Triton X-100 micelles in D_2O, the ϕ_Δ were more than 10 times lower. They suggested that the formation of $^1O_2$ in aerobic solution is limited, and this is mainly due to the low triplet state formation.[55]

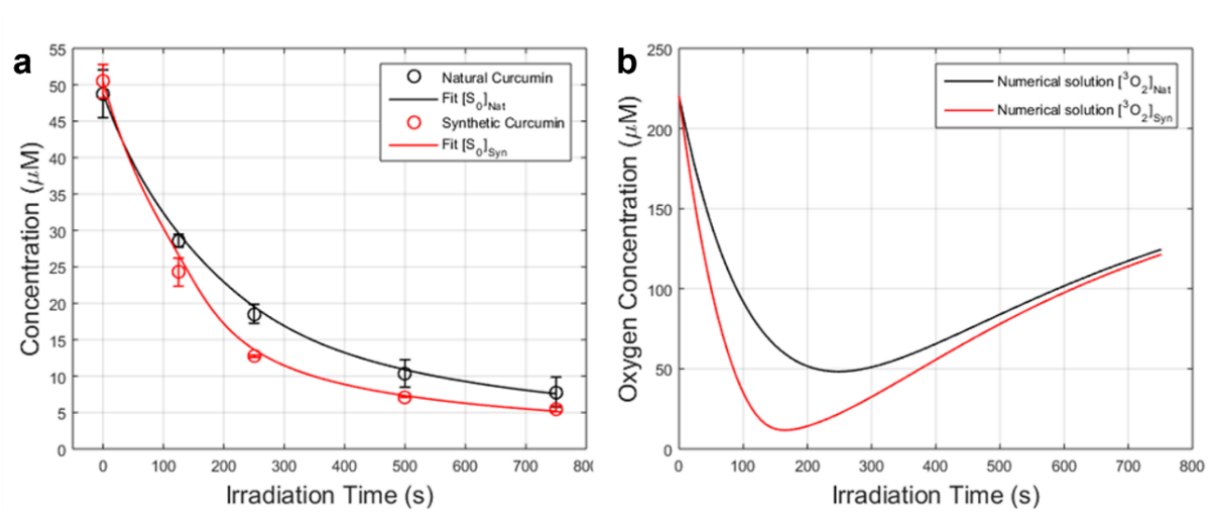

Figure 9 - (a) Concentration x Irradiation time at 464 nm for photobleaching experiment for curcumin and synthetic curcumin. (b) Oxygen concentration x Irradiation time for photobleaching experiment for curcumin and synthetic curcumin.

Source: By the author.

Table 4 - Table of fitted constants for the photobleaching of curcumin (N) and synthetic curcumin (S).

	$\phi_T I_a$ (s^{-1})	$k_{ta}[A]$ ($\mu M^{-1}s^{-1}$)	k_p (s^{-1})	k_{ot} (s^{-1})	$S_\Delta k_{ot}$ ($\mu M^{-1}s^{-1}$)	k_{os} ($\mu M^{-1}s^{-1}$)	$k_d + k_{oa}[A]$ (s^{-1})	k_d (s^{-1})	g ($\mu M/s$)	R^2	σ (cm^2)
N	0.185	1049.26	2077.8	3190.8	999.1	9.7	5670.6	1751.07	0.998	0.998	$4.2x10^{-17}$
S	0.122	1028.82	7323.9	1790.8	999.9	9.9	5510.9	454.76	0.998	0.997	$8.7x10^{-17}$

Source: By the author.

The effective irradiance can also be calculated as the result of the area under the curve of absorbance multiplied by the spectral irradiance of the Biotable® device used (Figure 10), as shown in equation (8). It will provide quantitative information of the energy available to the molecule for photodynamic effects.

$$I_{abs} = \int_{\lambda_1}^{\lambda_2} I_0(\lambda)(1 - e^{-\mathrm{abs}(\lambda)})\mathrm{d}\lambda \qquad (10)$$

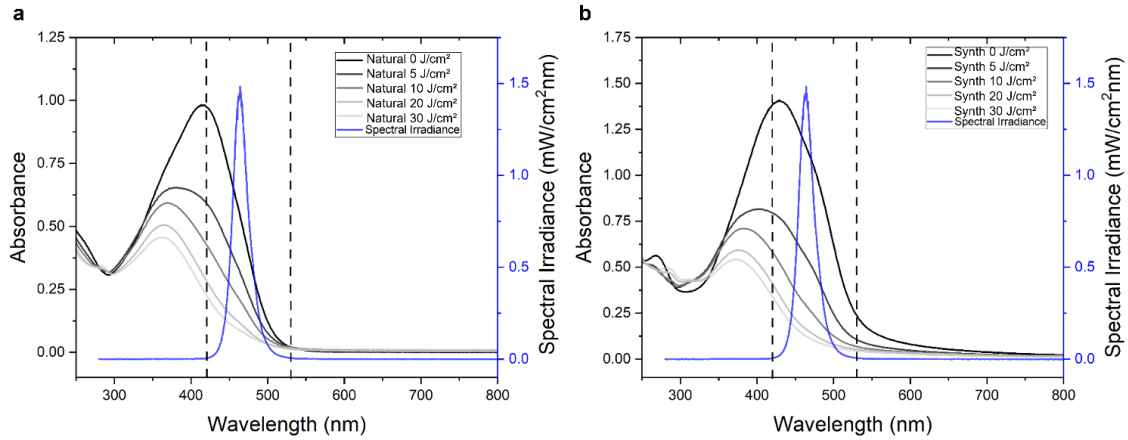

Figure 10 - Double-Y plot of curcumin absorbance and the Biotable®'s spectral irradiance at each fluence delivered. The wavelength area delimitated ranges from 415 to 575 nm. a. Natural curcumin b. Synthetic curcumin.

Source: By the author.

The result of this integral for each fluence and curcumin is presented in Figure 11, and the area integrated ranged from 415 to 575 nm, as indicated in Figure 10. It can be observed that synthetic curcumin absorbed more light at each fluence delivered than curcumin. The absorbed irradiance by synthetic curcumin was about 1.5 times higher than that for natural curcumin. This higher absorbed irradiance allows more

molecules to become available for the photodynamic effect, and eventually results in a faster decay of the molecule itself.

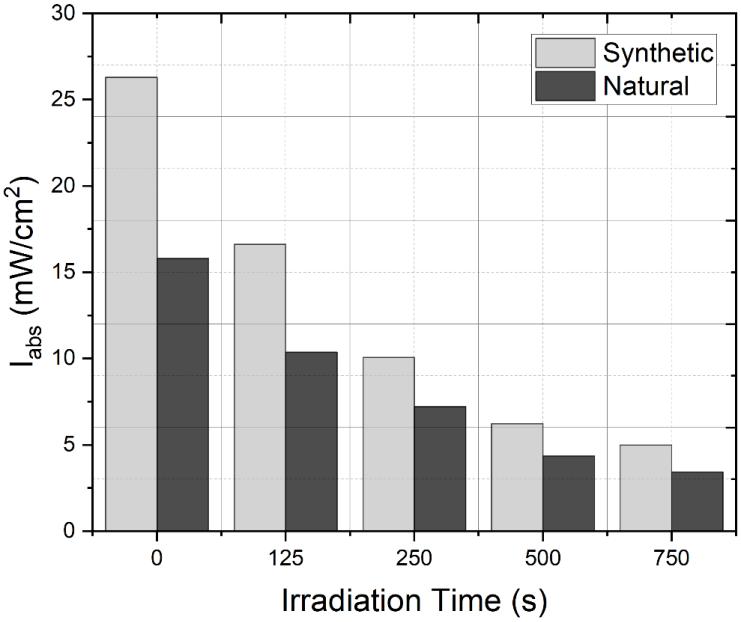

Figure 11 - Effective irradiance vs irradiation for curcumin and synthetic curcumin.

Source: By the author.

Despite having low solubility in water, curcumin has different solubilities in different organic solvents, such as DMSO. Thus, in these experiments, curcumin was initially prepared in DMSO to later be diluted in water. For both types of curcumin used, the absorption spectra recorded mainly consisted of a strong and broad peak in the 250 – 530 nm wavelength region. This suggests the presence of more than one oligomer in the ground state. The absorption maxima amplitude was found to be 415 nm for natural curcumin and 430 nm for synthetic curcumin, the differences seen on the maximum is due to differences in the composition of each curcumin. For the experiments reported here, the photobleaching of curcumin analysis was performed with an illumination system in a wavelength centered at 464 nm.

Regarding curcumin photodecomposition, Nardo *et al*.[59] showed that there was no dependance between singlet oxygen generation and photodegradation when using polar solvents such as acetonitrile and methanol. Priyadarsini (2009) suggested that the degradation occurs mainly through the break of the β-diketone bond forming smaller phenolic compounds, a mechanism independent of the presence or absence of the phenolic group OH in the curcumin molecule.[45]

Our results showed that synthetic curcumin presented an absorbed irradiance 1.5 times higher than natural curcumin; this behavior is present in all fluencies delivered. Therefore, synthetic curcumin is expected to have a faster photodegradation than natural curcumin as observed in Figure 9(a). Regarding the ϕ_T, natural curcumin is 3.1 times higher than that of synthetic curcumin (0.047 and 0.015 respectively), meaning that, the natural will have a higher population that can eventually generate an energy transfer reaction to the molecular oxygen and then generate type II pathway compared to the synthetic curcumin.

This hypothesis can be better understood by the fitted values of ϕ_Δ, which is one order of magnitude bigger for natural than the synthetic curcumin (0.015 and 0.008 respectively).

2.3.3 Photodynamic Inactivation

Considering the positive effects PDI shows in killing bacteria cells, understanding and optimizing its effectiveness is key to better utilize photosensitizing molecules in smaller amounts and to find alternatives that are more easily obtained, via synthesis, and more environmentally friendly while also being as effective as its natural counterpart. As such, comparing photodynamic action of curcumin and its synthetic analogue is an important step in optimizing curcumin-mediated PDI.

Firstly, a plethora of conditions were tested for both curcumin and synthetic curcumin, changing concentration and fluence to compare reduction in colony-forming units in a logarithmic scale. Groups shown below include control groups: CON (bacteria only), C (curcumin concentration in μM), L (light irradiation in J/cm²); as well as treatment groups: CL groups (PDI).

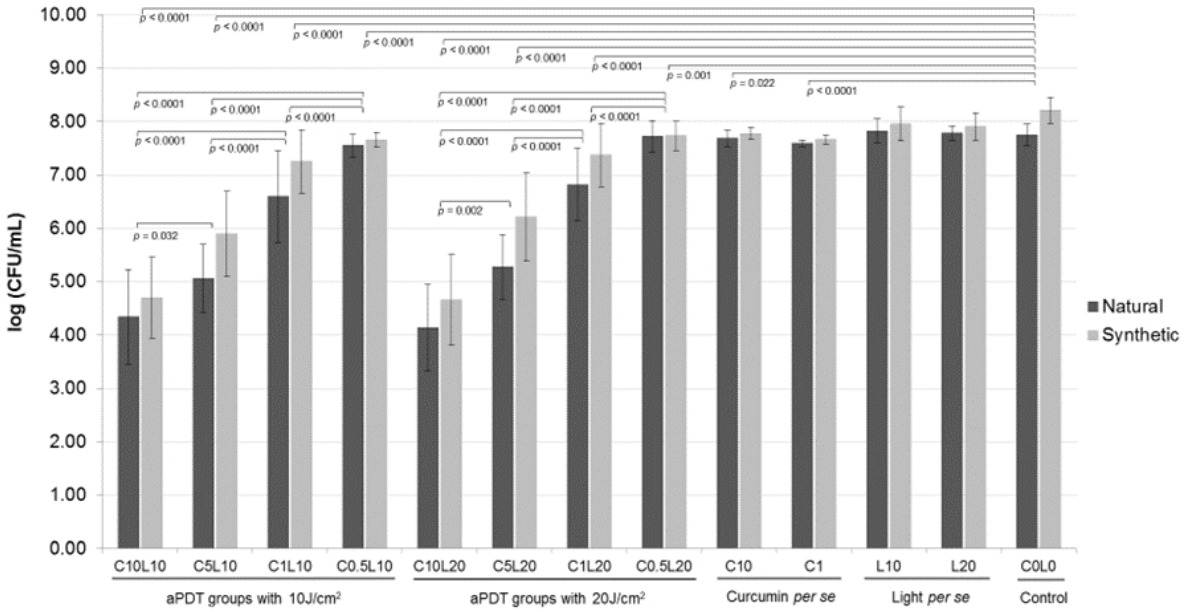

Figure 12 - Antimicrobial Photodynamic Therapy inactivating *S. aureus* using curcumin and its synthetic analogue at concentrations (shown as 'C') 0,5; 1; 5; and 10 μM and illuminating at 10 and 20 J/cm² fluencies (shown as 'L'), aPDT groups have both of them. Columns and error bars represent the mean values and standard deviation of log (CFU/mL), respectively. Comparison between natural versus synthetic curcumin showed statistically significant differences, regardless of treatment group (ANOVA: $p < 0.0001$). Treatment group also promoted a significant effect (ANOVA: $p < 0.0001$) and the statistically significant differences between two means are indicated with the brackets and respective p values from Games-Howell post-hoc test.

Source: By Dr. Lívia Dovigo.

Two-way ANOVA indicates that both type of curcumin and treatment groups promote significant effects in log (CFU/mL), with the former having a low effect size ($\eta^2p = 0.12$) and the latter having a much larger effect size ($\eta^2p = 0.86$) and interaction between the two did not show significant effect in reducing log (CFU/mL).

Regardless of fluence, all treatment groups showed significant reduction in log (CFU/mL) values compared to control groups ($p < 0.001$). All four concentrations tested showed different reduction values, indicating that response is somewhat concentration-dependent, with the 10 μM concentration presenting the biggest reduction (3.52 and 3.40 for natural and synthetic curcumin, respectively).

S. aureus PDI studies using curcumin are well documented in the literature, several authors have described its effectiveness. Freitas *et al.*[25] tested PDI on both *S.aureus* ATCC 25923 and MRSA, obtaining 4 logs reduction while using 100 μg/mL

of curcumin and illuminating with fluencies of 8 and 20 J/cm², demonstrating the technique's ability to inactivate this Gram-positive bacteria as well as a resistant strain.

Santos *et al.*[60] evaluated curcumin-mediated PDI effects in MRSA using 100 µg/mL curcumin and a 54 J/cm² fluence, obtaining complete inactivation of that bacterial stain.

Our results showed that curcumin-mediated PDI with 10 µM curcumin produced satisfying results by inactivating up to 3.52 logs, and 5 µM test groups inactivated up to 2.69 logs. These results are in accordance with other studies and while the type of curcumin showed a statistically significant effect on log (CFU/mL) values (ANOVA: $p < 0.010$) it is of low effect size. In general, the usage of naturally occurring curcumin showed slightly higher reduction values than its synthetic analogue, with the greatest mean difference occurring in the C5L20 group (0.9 log). However, the low effect size coupled with the fact that difference between curcumins did not reach 1 log indicate that little practical significance is observed considering this effect.

Moreover, light dose (10 or 20 J/cm²) had no significant effect on the PDI result itself (Games-Howell: $p \geq 0.309$) though different concentrations of curcumin produced different reduction levels in a concentration-dependent manner.

Increasing fluence is also an important factor for PSs as it generates more singlet oxygen, therefore enhancing photodynamic inactivation [55]. However, as evidenced by our work, in this specific environment, curcumin reached its peak photodynamic activity in mere 10 J/cm² and the different fluencies had no significant effect on the PDI result itself (Games-Howell: $p \geq 0.309$). This effect could be explained through the oxygen photo-consumption plot obtained, which shows a minimum at around 165.4 and 248.7 s, which corresponds to 6.62 J/cm² and 9.95 J/cm² for synthetic and natural curcumin, respectively. The difference between these fluencies can be explained with the absorbed irradiance in Figure 11 and the S_Δ, which is the fraction of $[T]$ and $\left[{}^3O_2 \right]$ reaction that produce $\left[{}^1O_2 \right]$.

In general, mechanisms of action that lead to bacterial cell death are well understood, PDT targets bacteria's cytoplasmic membrane, macromolecules like proteins and lipids, and DNA [61]. As such, PS uptake is important for generating ROS inside the bacterial cell, resulting in higher inactivation and concentrations used which can be attributed to an accumulation of curcumin inside the cell or surrounding it.[62] Our results show that an increase in concentration is directly related to an increase in cell death [62]. It is estimated that 20 minutes is enough time for curcumin incubation as no

change was observed by increasing that time (data not shown) which is also backed up by fellow researchers[25, 63]. Parameters essential to the success of this technique have been tested for both curcumins used, analyzing, and validating the use of synthetic curcumin for application.

Synthetic photosensitizers have been used in PDT for some time and curcumin is no exception. A synthetic analogue can be prepared in moderate quantities and this approach could be a viable alternative to the use of natural curcumin as it is less costly, more sustainable, and environmentally friendly[48, 50] while also bypassing purity and concentration issues present in natural curcumin since soil conditions affect its contents, as previously stated.

Below a schematic was made to illustrate the possible interactions and energy transfers that happen. After being irradiated and absorbing energy to reach a triplet state, the curcumin molecule can either transfer that energy to another ground-state curcumin or to molecular oxygen. Afterwards, the singlet oxygen generated can oxidate curcumin molecules, degrading them as evidenced by the UV-vis spectra (Figure 7), or interacting with the many biological targets in bacteria, promoting its death.

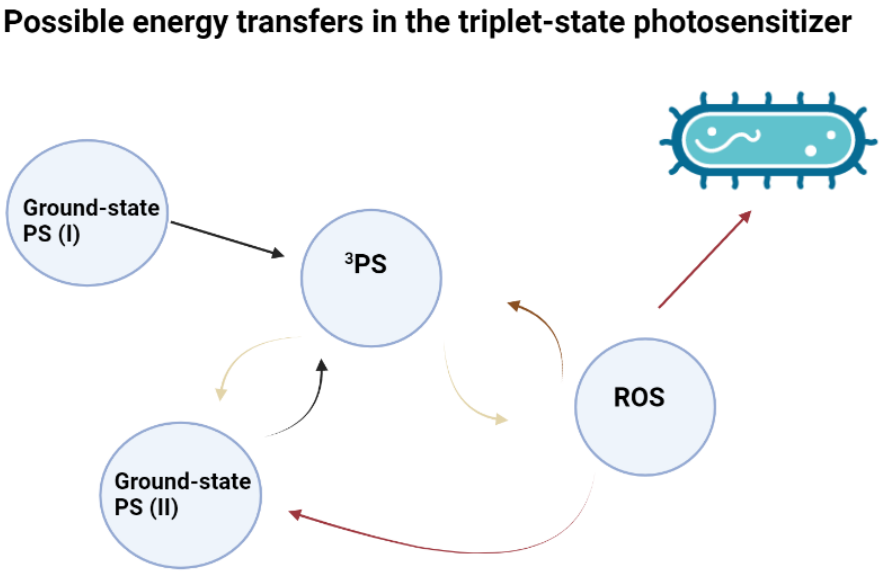

Figure 13 - Possible interactions and energy transfers with the excited photosensitizer. Arrows in yellow represent energy transfer while arrows in red represent oxidation inducing damage/degradation.

Source: By the author.

2.4 Conclusion

Both curcumin and its synthetic analogue share similar photobleaching and aPDT results. Synthetic curcumin consumes oxygen more rapidly and degrades faster than naturally occurring curcumin, and though singlet oxygen generation is quite low compared to other photosensitizers (0.015 for natural curcumin and 0.008 for synthetic curcumin), when comparing both curcumins, the natural one has higher triplet quantum yield (0.047) than the synthetic one (0.015). aPDT results against *S.aureus* showed that inactivation increased based on the concentration, with a reduction up to 3.52 logs when using 10 µM of curcumin which is considered great as it represents more than 99.9% bacteria reduction, meanwhile fluence had no effect in that. When comparing the type of curcumin used, differences did not reach 1 log. Thus, usage of the synthetic molecule is a great choice considering it being less costly, environmental-friendly, and easier to characterize while maintaining its effectiveness in PDT.

3 EVALUATING SYNTHESIZED CURCUMINOIDS AND THEIR MIXTURE AS PHOTOSENSITIZERS IN PDI

3.1 Context

As it is known, naturally occurring curcumin is a mixture of curcuminoids and terpenoids. The content of each curcuminoid in the rhizome of *C. longa* varies with soil conditions and the age of the root. This makes it difficult to recreate protocols using curcumin in a clinical environment. A better understanding of each curcuminoid pigment individually and the mixture of all three may help elucidate such questions.

3.2 Materials and methods

3.2.1 Curcuminoid preparation

For the preparation of the curcuminoids, 8.25 mg of DMC (Molecular weight: 338.4 g/mol) and 7.55 mg of BDMC (Molecular weight: 308.3 g/mol) were dissolved in DMSO (5 mL) in a centrifugation tube for a stock solution of 4.886 mM. Dilution for experiments was done in distilled water, the same way as with curcumin for a final concentration of DMSO < 0.1%.

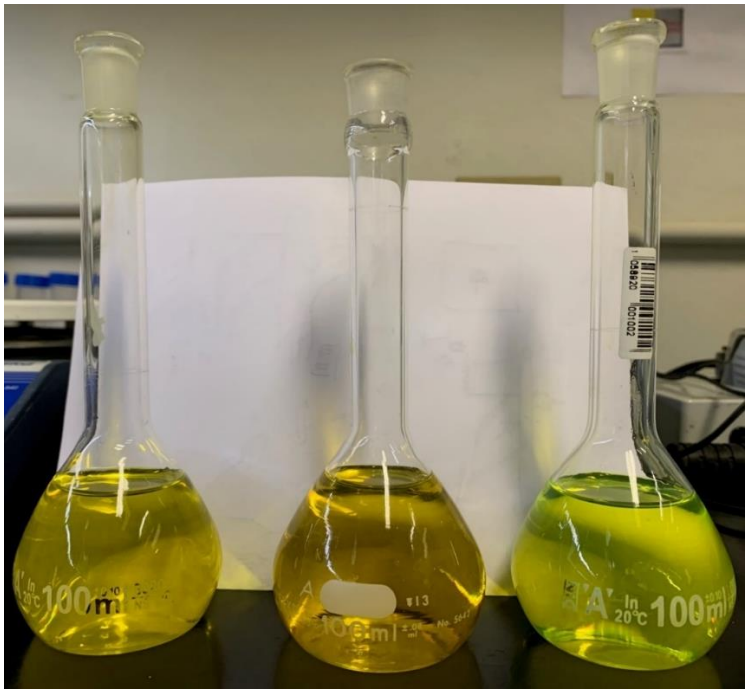

Figure 14 - All three curcuminoid solutions. From left to right: curcumin, DMC, and BDMC. Solutions not made following described procedure, for illustration purposes only.

Source: By the author.

3.2.2 Fluorescence spectroscopy

To measure each curcuminoid emission spectrum, a fluorimeter (Cary Eclipse Fluorescence Spectrometer) was used. Each curcuminoid was prepared at 50 μM and excited at 430 nm since they all possess a characteristic peak that covers that wavelength. Fluorescence intensity and wavelength distribution of emission spectrum was measured from 450 to 750 nm with steps of 10 nm per measure of emission intensity.

3.2.3 Fourier-transform infrared spectroscopy (FTIR)

Using the infrared spectroscopy is yet another way to check whether the curcumin powders is in fact curcumin since the absorption peaks revealed after light absorption represent the molecular vibrations of functional groups within the sample. IR spectra were recorded using the Cary630 FTIR Agilent Technologies spectrometer. Curcumin, synthetic curcumin, DMC, and BDMC powders were crushed and used for spectrum reading.

3.2.4 Photodynamic Inactivation

PDI studies were carried out for the other two curcuminoids DMC and BDMC following the same protocol as explained in section 2.2.4. For this set of experiments, the same strain of *S. aureus* ATCC 25923 was used. Synthetic curcumin was used to compare its response to the new PDI groups using curcuminoids DMC and BDMC.

Six different mixtures of the three curcuminoids were tested by permutating the content of each curcuminoid as found in the natural curcumin used in the previous experiment. Natural curcumin's curcuminoid content was analyzed by HPLC in a previous study[23] and it is found in Table 5 (Mixture 1).

Table 5 - Mixture of the three curcuminoids based on the proportion found on the natural curcumin used (Mixture 1).[23] For easier viewing, mixtures 2-5 had their contents percentage rounded.

	Curcumin (%)	**DMC (%)**	**BDMC (%)**
Mixture 1	**57.649**	**16.356**	**25.995**
Mixture 2	58	26	16
Mixture 3	26	57	16
Mixture 4	26	16	58
Mixture 5	16	26	58
Mixture 6	16	58	26

Source: By the author

3.2.5 Statistical analysis

Each group was tested in triplicate in three different occasions (n=9). When analyzing PDI groups containing the proposed mixtures (Table 5) and performing descriptive analysis and checking assumptions of normality and homoscedasticity, an analysis of variance was performed with Welch's t-test, followed by Tukey post-hoc test. Significance level was set at 0.05.

3.3 Results and discussion

3.3.1 Spectrophotometer spectra

Both DMC and BDMC had their UV-vis spectra measured using the spectrophotometer and at a concentration of 50 µM. A photobleaching study was also performed at the same fluencies as curcumin using the same illumination device, Biotable. Qualitatively, it can be said that their photobleaching pattern resembles that of curcumin, showing signs of aggregation through blue-shift although BDMC has lesser decrease in its absorbance than the other curcuminoid pigments.

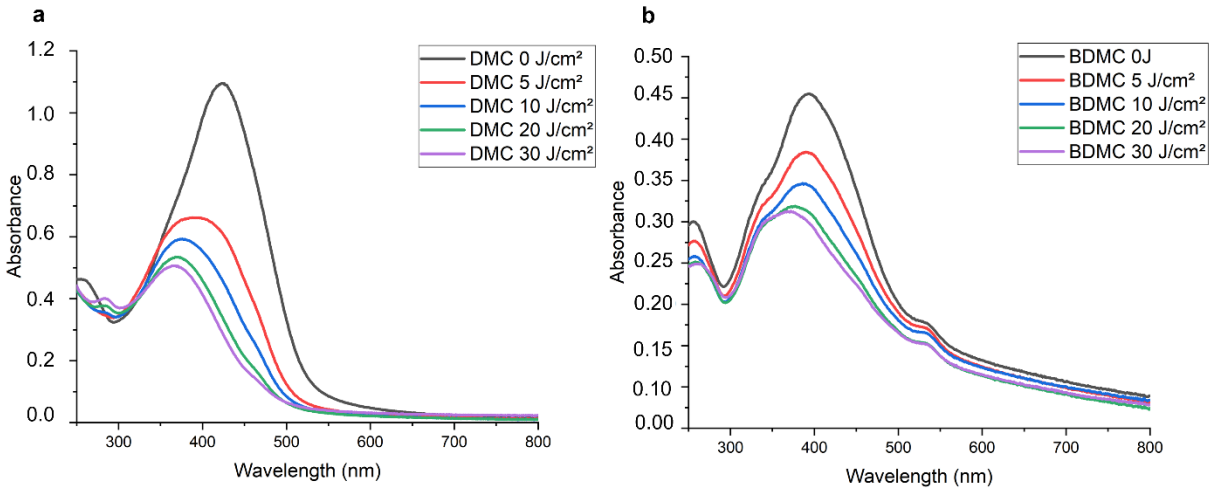

Figure 15 - Photobleaching pattern for DMC (a) and BDMC (b). Concentration for both pigments was 50 µM and fluencies used were 5, 10, 20, and 30 J/cm².

Source: By the author.

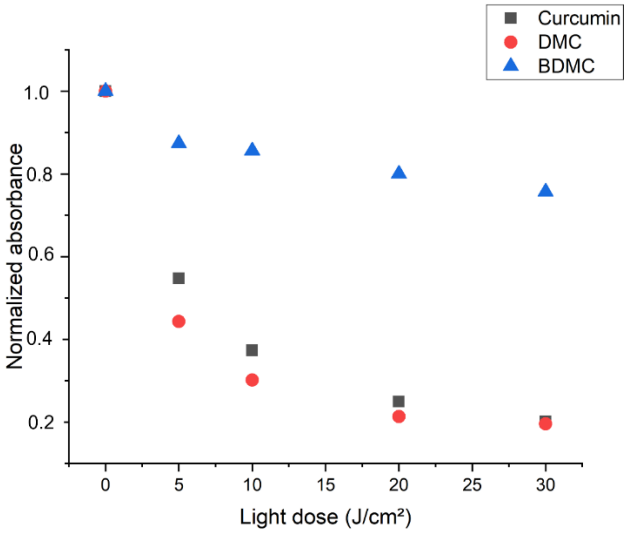

Figure 16 - Peak absorbance decrease over photobleaching action on curcumin, DMC, and BDMC.

Source: By the author.

Following the absorption spectra, samples were excited at 430 nm in the fluorimeter and the fluorescence emission spectrum showed peak emission near 560 nm for all four pigments (Figure 17) and, remarkably, BDMC emitted about 5 times more fluorescence than the other curcuminoids.

Given BDMC's apparent photostability as shown in Figure 16 coupled with its fluorescence emission, we can hypothesize that it emits more fluorescence than curcumin and DMC because it is less degradable under light excitation. This also expands BDMC's usage as it could be potentially used as a marker in diagnosis, this dual effect is also seen in the fluorescent dye rhodamine which is widely used in the development of new photosensitizers as a fluorophore moiety while also displaying great photophysical and chemical properties for PDT.[64] *Zhang et al*.[65] developed and tested a fluorescent PS that has the advantage of also being used in imaging bacteria without the need of a washing process, killing the bacteria via image-guided PDT. Further studies with BDMC could lead to interesting and different new uses compared to curcumin and DMC due to the photophysical properties discovered.

According to Ali *et al.*[66], the fluorescence emission for curcuminoids range from 548 to 575 nm, depending on the concentration of curcumin. In their study, the levels of curcuminoids in turmeric bought in local markets were compared by using fluorescence spectroscopy, although the whole turmeric was excited at 467 nm and, in our experiment, only the curcuminoids were excited. Nevertheless, the emission spectrum obtained is in agreement with the one reported and is indicative that the curcuminoids used in further PDI experiments are in fact authentic.

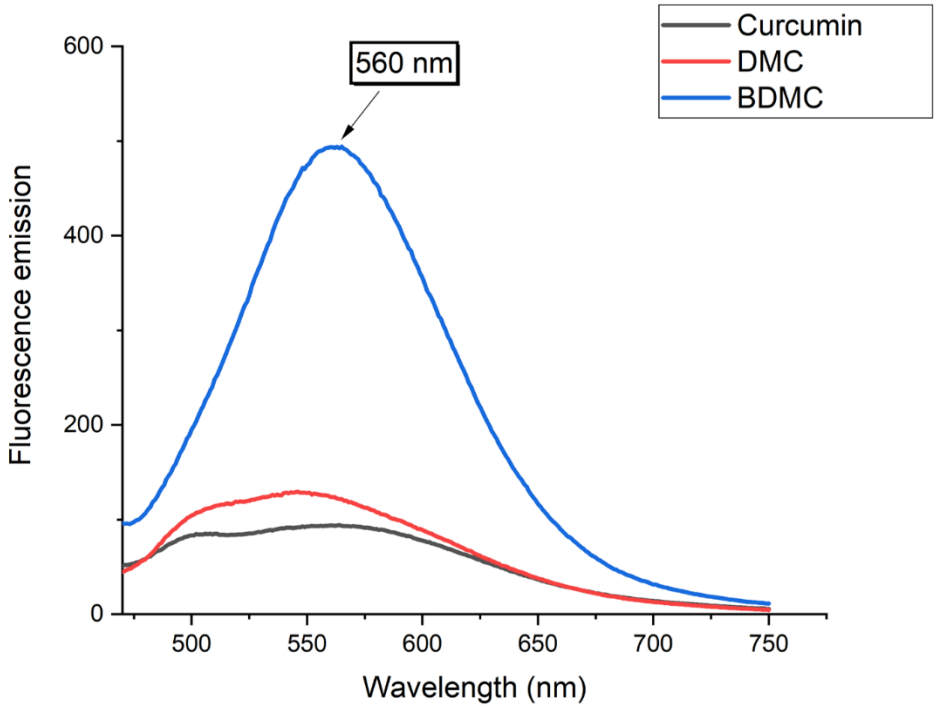

Figure 17 - Fluorescence emission spectra for each curcuminoid at 5μM. Samples were excited at 430 nm and emission recorded ranged from 450 to 750 nm.

Source: By the author.

FTIR spectra was also obtained to check the samples used and curcumin has characteristic peaks that can be identified with precision. In Figure 18 the absorption spectra of all four powder samples utilized are shown, including curcumin signature peaks marked by the wavenumber.

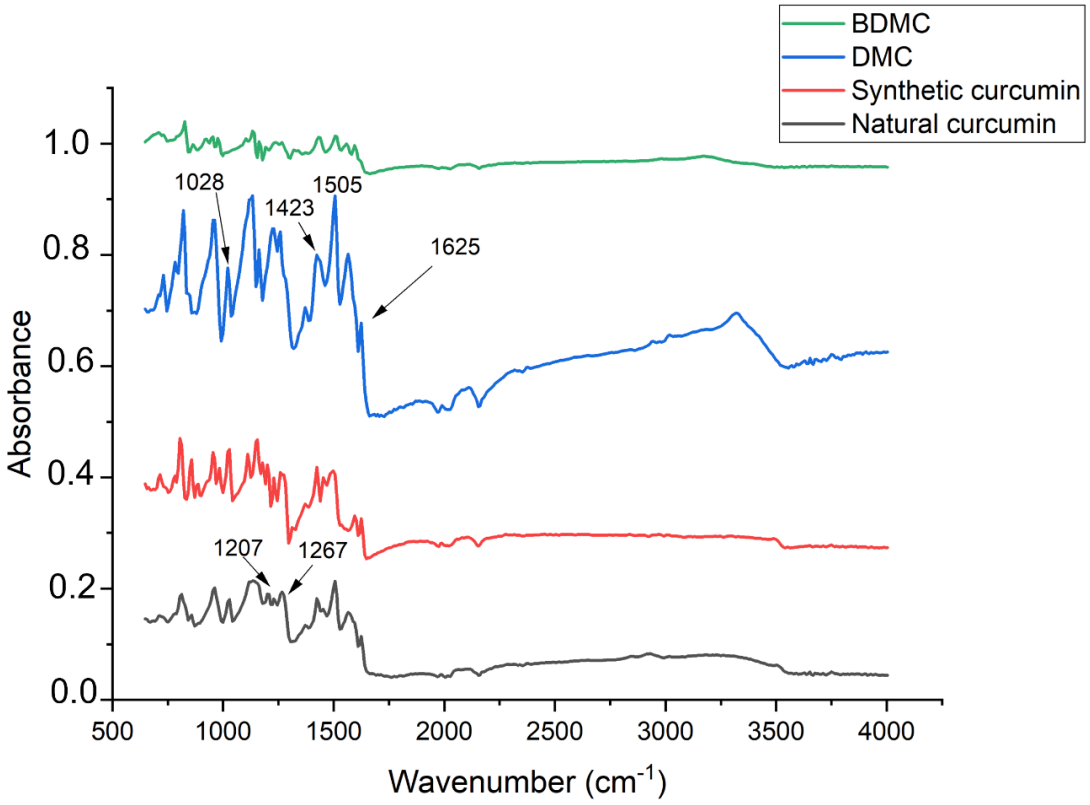

Figure 18 - FTIR spectra of curcumin (black), synthetic curcumin (red), DMC (blue), and BDMC (green). Source: By the author.

Relevant peaks related to functional groups in curcumin were found at 1625 cm^{-1} (overlapping cyclic alkene C=C and carbonyl C=O stretching), 1505 cm^{-1} (aromatic skeletal stretching), 1423 cm^{-1} (C=C aromatic stretching vibration), 1267 cm^{-1} (C-O phenolic band vibration), 1207 cm^{-1} (C-O ether stretching) and, 1028 cm^{-1} (C-O-C stretching vibration). Of which, only peaks at 1207 cm^{-1} and 1028 cm^{-1} were not found in BDMC, which are associated with ether and C-O-C stretching vibrations, that is noteworthy, given that BDMC is the only one without a methoxy functional group, as opposed to curcumin and DMC which contain at least one. As Chen *et al.*[67] have also reported, curcumin has signature peaks in wavenumbers close to those obtained even when encapsulated in nanoliposomes or phospholipids, demonstrating the preciseness of the FTIR technique in identifying samples.

Given all spectroscopy-based results, it is safe to assume that the curcumin and curcuminoids used in all following experiments are authentic and synthesized well and possess all functional groups present in the molecular structure. Usually NMR is the more commonly used technique to characterize compounds, these results can be found in Carmona's article on the synthesis of curcuminoids.[48] Since this work's

objective is to use these pigments in PDI, an optical approach to characterization is fitting to better understand how these PSs could differ when given the light dose.

3.3.2 Photodynamic Inactivation

As concluded in section 2.3.3, light dose for PDI experiments was set to 10 J/cm² and incubation time at 20 minutes. As such, each curcuminoid was tested at concentrations 10, 1, and 0.75 µM. CFU were counted the day following the experiment and is presented in Figure 19.

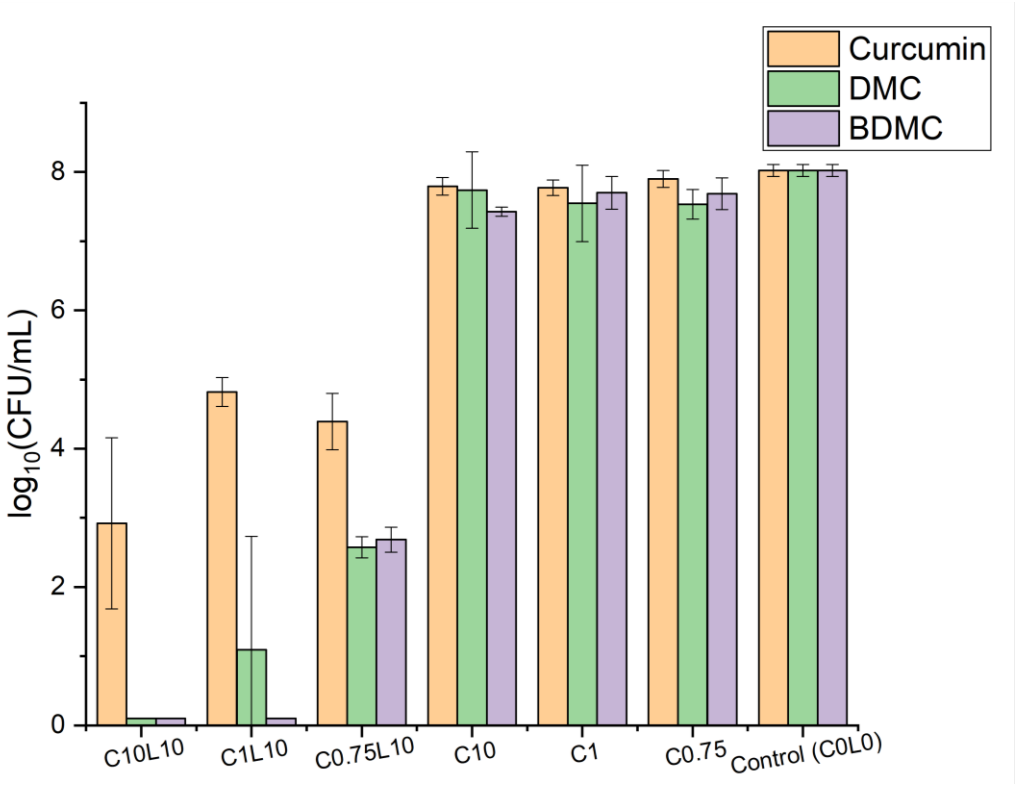

Figure 19 - PDI results against S.aureus using each curcuminoid individually. Concentrations (C) ranged from 10 - 0.75 µM and light dose (L) used was 10 J/cm².

Source: By the author.

In this first preliminary experiment, we can observe that curcuminoids DMC and BDMC consistently inactivate more *S. aureus* logs than curcumin, though it is notable that all groups differ from control groups which indicate that all three were successful in killing the planktonic bacteria.

Following the same principle, mixture 1 (Table 5) of the curcuminoids was tested in PDI in a range of concentration from 10 – 0.10 µM, since it was expected that the inactivation with all three molecules would be better than the isolated curcuminoids.

This set of experiments helped determine a single concentration to be used when using the different proposed mixtures.

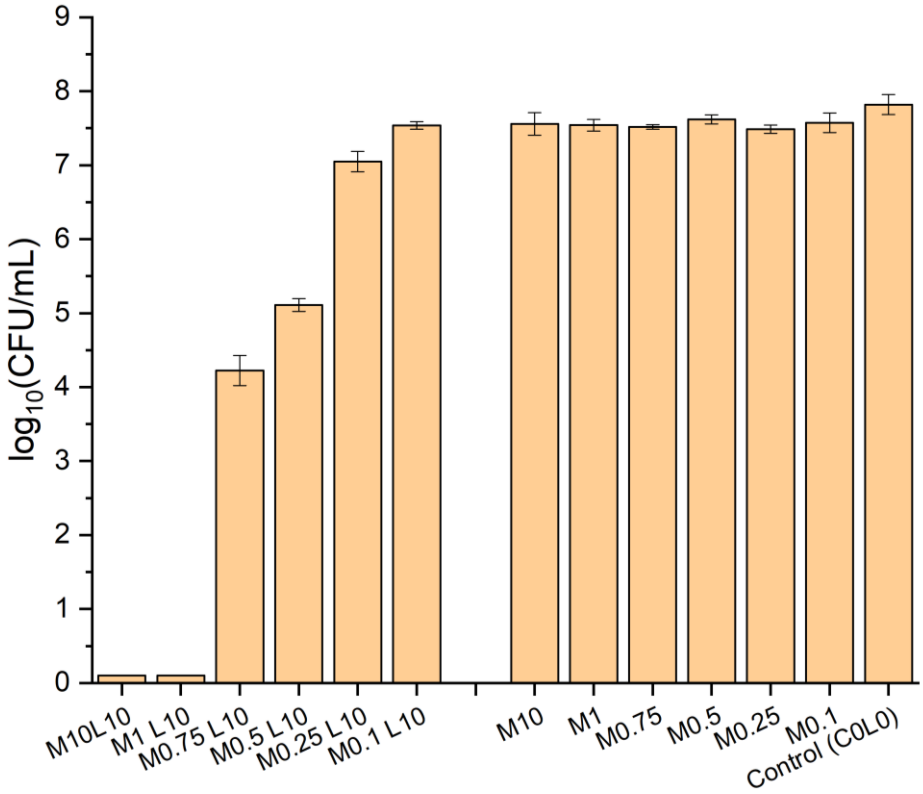

Figure 20 - PDI results against S.aureus testing mixture 1 (Shown as 'M') in different concentrations that ranged from 10 - 0.1 µM. Light dose (L) was set at 10 J/cm².

Source: By the author.

Here it can be noticed that inactivation using the curcuminoid mixture is mediated in a concentration-based pattern, similar to results found in the studies comparing natural and synthetic curcumin (Section 2.3.3). Moreover, it is also interesting that PDI groups using 10 and 1 µM completely inactivated *S.aureus* while curcumin by itself (Figure 19) only partially inactivated the bacteria which could at first glance suggest that the joint action of DMC and BDMC enhance photodynamic activity.

After establishing concentration (0.75 µM), light dose (10 J/cm²) and incubation time (20 minutes) the remaining mixtures (see Table 5) were tested under those conditions and statistical analyses were carried out as to better understand the differences seen in PDI effectiveness.

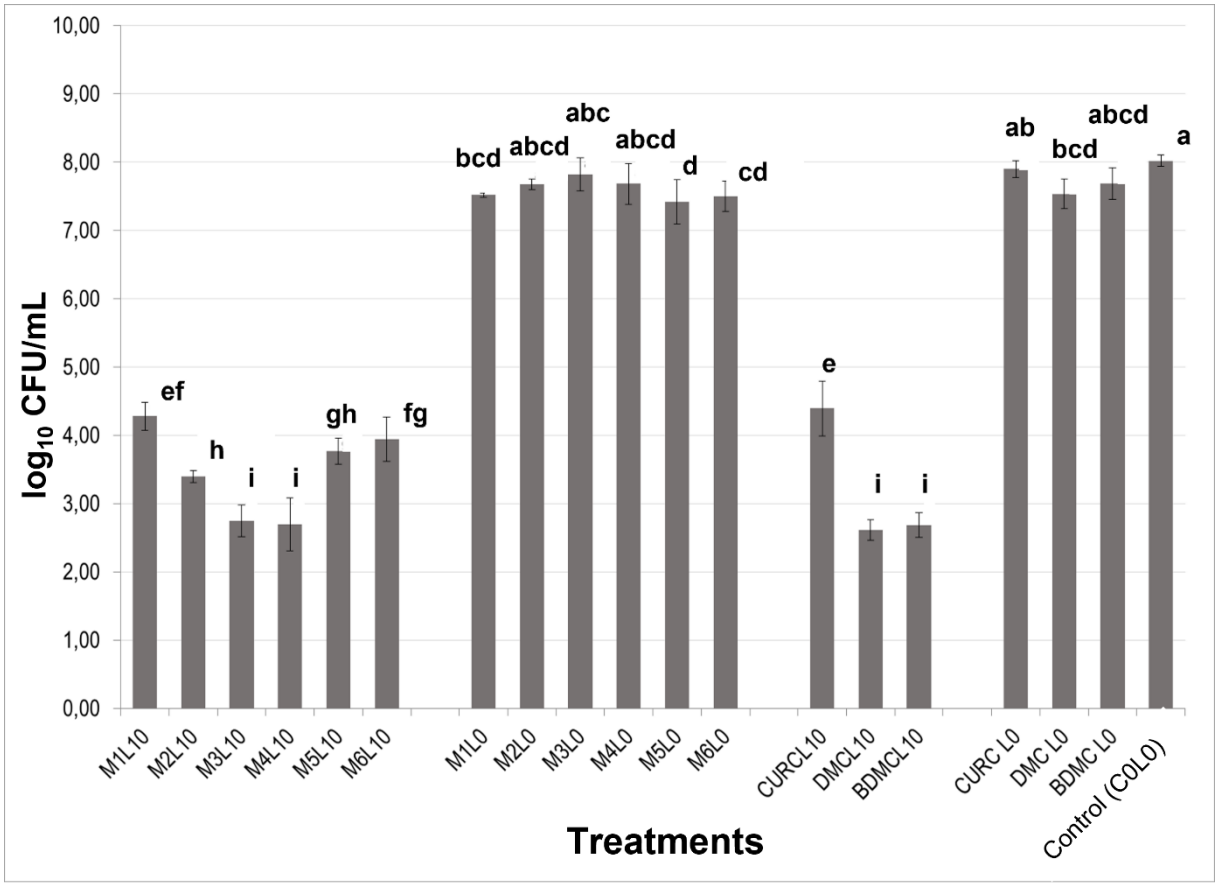

Figure 21 - Mean values and standard deviation of log_{10}(CFU/mL) of PDI and control experiments with S. aureus using mixtures (M) of curcuminoids and each isolated curcuminoid. Light dose (L) was set at 10 J/cm² for all PDI groups. Different letters indicate statistically different means between groups.

Source: By Dr. Lívia Dovigo.

As expected, treatments using only the curcuminoids and not irradiating light were generally incapable of inactivating the bacteria, although DMC and mixtures 1, 5, and 6 differed statistically from the control group, the difference in log_{10}(CFU/mL) was only 0.5. PDI treatments were all able to inactivate the bacteria though mixtures 3 and 4 were the most efficient and isolated curcuminoids DMC and BDMC both reduced more than 5.0 logs, in comparison curcumin reduced 3.63 logs.

This finding could inspire future studies on PDI as both DMC and BDMC can be synthesized in large quantities and *in vitro* results showed that they are more efficient than curcumin. Mixing the three curcuminoids together might affect their overall efficiency as a PS. However, it does not seem like mixing them produce better results than using DMC or BDMC individually. It can be hypothesized that an energized species may transfer its energy to another instead of molecular oxygen, though oxygen

singlet quantum yield for each molecule would have to be researched in depth as to confirm this.

In research made by *Young et al*.[68] tested the three curcuminoids against three pathogenic fungi of the *Colletotrichum* genus, these fungi are responsible of causing anthracnose and they tested each curcuminoid's potential as an antifungal substance. They discovered that *in vitro* all three curcuminoids significantly inhibited mycelial growth in concentrations as low as 4 µg/mL when testing against *C. coccodes, C. acutatum*, and *C. gloeosporioides*. Meanwhile, *in vivo* testing on red pepper plants showed that only DMC had antifungal activity in a concentration of 500 and 1000 µg/mL. Additionally, no phytotoxicity was found against the red pepper plants even in concentrations as high as 2000 µg/mL.

In another study conducted by *Hung et al*.[69] DMC and BDMC were synthesized and approximately 3µM of each PS was tested in PDI against *Staphylococcus epidermidis* and *S. aureus*, illuminating for 1 min under a 3.0 mW/cm² blue light. They reported that while curcumin killed 14.1% of a 10^9 bacteria sample, both DMC and BDMC killed nearly all bacteria present. This finding is in accordance with what we discovered, although the exact reason as to these curcuminoids enhanced photodynamic activity is still unknown.

Although not much is reported on DMC and BDMC's potential as a PS for PDI, researchers have studied DMC's antitumor potential against different types of cancer, such as brain, ovarian, breast, lung, prostate, and skin cancer.[70] Xin *et al*.[71] also reported that combining 40 µmol/ L of DMC and irradiating 60 mJ/cm² of UV-B enhanced apoptosis *in vitro* against A431 cells for cutaneous squamous cell carcinoma by killing up to 35% of cells. On the other hand, *Wu et al*.[72] conducted a study on the same cell line and treating it with curcumin to assess its cytotoxic effects and concentrations of 15 µmol/L inhibited up to 60% of A431. It was checked that curcumin inhibited expression of the signal transducer and activator of transcription factor 3 (STAT3) which is a key molecule in the malignant transformation of cells. Given these differing reported results, more information is needed to establish DMC as an alternative to the more commonly used curcumin in carcinoma treatments.

3.4 Conclusion

Through optical techniques the absorbance and fluorescence emission of each curcuminoid was evaluated as well as its functional groups through FTIR. With PDI experiments it was possible to completely inactivate *S. aureus* using DMC and BDMC with concentrations as low as 1 µM and with 0.75 µM they were in general more efficient than curcumin in inactivating *S. aureus* (5.41 and 5.34 logs for DMC and BDMC, respectively, and 3.63 logs for curcumin), meanwhile the initial hypothesis that the mixture of curcuminoids could improve photodynamic therapy was proven when comparing to curcumin by itself. Most mixtures, excluding mixture 1 (57% CUR, 16% DMC, 27% BDMC), were statistically different to curcumin and inactivated more than 4.08 logs. However, even the most efficient mixtures, 3 (27% CUR, 57% DMC, 16% BDMC) and 4 (27% CUR, 16% DMC, 57% BDMC), were able to kill *S. aureus* to levels comparable to DMC and BDMC individually, all reducing up to 5.41 logs. Thus, the use of these PSs in PDT could serve as inspiration to future works and opens new perspectives on the use of curcuminoid pigments, as its synthesis can be done in a large scale and is more environmentally friendly.

4 GENERAL CONCLUSIONS

In this study the differences between natural curcumin and a synthetic analogue as well as the effects of curcuminoids DMC and BDMC in PDI against *S. aureus* were explored. Since curcumin is widely used as a photosensitizer in our research group, CEPOF, the better understanding of photophysical properties of curcumin and a cheaper, pure, and environmentally friendly synthetic analogue is paramount to its usage not only against microorganisms *in vitro* but also in more advanced studies *in vivo*.

As such, through photobleaching studies it was found that there are differences between curcumin and synthetic curcumin in their singlet oxygen generation and their degradation rates, though that difference was not noticeable when testing in PDI studies. It was also concluded that using higher fluencies than 10 J/cm² did not improve the inactivation of *S. aureus*, but it follows a concentration-dependent pattern. Thus, higher concentrations of curcumin yielded better results.

Another interesting conclusion was reached after testing curcuminoids DMC and BDMC and discovering their potential in PDI when compared to curcumin, not only due to their molecular similarity, but also due to their overall similar photophysical parameters such as absorbance and fluorescence (apart from BDMC).

The hypothesis that a combination of curcuminoids would enhance photodynamic activity was somewhat proven when comparing their log (CFU/mL) reduction to curcumin. However, even the best mixtures for PDI reduce bacteria population to levels similar to DMC and BDMC by themselves.

In conclusion, the objectives of this study were met and results open new future perspectives to the use of curcuminoids in PDI, not only by validating the use of pure synthetic molecules but also expanding the pool of available PSs that can be used in treatments in more complex biological environments.

REFERENCES

1 ASLAM, B. *et al*. Antibiotic resistance: a rundown of a global crisis. **Infection and Drug Resistance,** v. 11, p. 1645-1658, 2018. ISSN 1178-6973 (Print) 1178-6973. DOI: 10.2147/IDR.S173867.

2 PRESTINACI, F.; PEZZOTTI, P.; PANTOSTI, A. Antimicrobial resistance: a global multifaceted phenomenon. **Pathogens and Global Health,** v. 109, n. 7, p. 309-18, 2015. ISSN 2047-7724 (Print) 2047-7724.

3 DADGOSTAR, P. Antimicrobial resistance: implications and costs. **Infection and Drug Resistance,** v. 12, p. 3903-3910, 2019. ISSN 1178-6973 (Print) 1178-6973. DOI: 10.2147/IDR.S234610.

4 PRESCOTT, L. M. *et al*. **Microbiology**. New York: McGraw-Hill, 2008. ISBN 9780072992915 0072992913.

5 MADIGAN, M. T.; BROCK, T. D. **Brock biology of microorganisms**. Boston [Mass.]: Benjamin Cummings, 2012. ISBN 0321778359 9780321778352 032164963X.

6 BUSH, L. Staphylococcus aureus infections. **Merck Manual**, 2019. Available from: https://www.merckmanuals.com/home/infections/bacterial-infections-gram-positive-bacteria/staphylococcus-aureus-infections. Accessible at: 12 Mar. 2021.

7 VOUGA, M.; GREUB, G. Emerging bacterial pathogens: the past and beyond. **Clinical Microbiology and Infection** : the official publication of the european society of clinical microbiology and infectious diseases**,** v. 22, n. 1, p. 12-21, 2016. ISSN 1469-0691 1198-743X. Available from: https://pubmed.ncbi.nlm.nih.gov/26493844. Accessible at: 12 Mar. 2021.

8 ANTIBIOTIC resistance threats in the United States, 2019. Atlanta, GA, 2019. Available from: https://stacks.cdc.gov/view/cdc/82532. Accessible at: 03 June 2020.

9 SOMMER, M. O. A. *et al*. Prediction of antibiotic resistance: time for a new preclinical paradigm? **Nature Reviews Microbiology,** v. 15, n. 11, p. 688-695, Nov. 2017. ISSN 1740-1526.

10 RESISTANCE, R. O. A. **Tackling drug-resistant infections globally**: final report and recommendations. 2016. Available from: https://books.google.com.br/books?id=aa6lAQAACAAJ. Accessible at: 23 March 2020.

11 LIVERMORE, D. M. *et al*. Discovery research: the scientific challenge of finding new antibiotics. **Journal of Antimicrobial Chemotherapy,** v. 66, n. 9, p. 1941-1944, 2011. ISSN 0305-7453. Available from: https://doi.org/10.1093/jac/dkr262. Accessible at: 8 Oct. 2022.

12 WORLD HEALTH ORGANIZATION. **2020 Antibacterial agents in clinical and preclinical development**: an overview and analysis**.** Geneva. 2021

13 GHORBANI, J. *et al*. Photosensitizers in antibacterial photodynamic therapy: an overview. **Laser Therapy,** v. 27, n. 4, p. 293-302, 2018. ISSN 0898-5901 1884-7269. Available from: https://pubmed.ncbi.nlm.nih.gov/31182904. Accessible at: 26 Apr. 2020.

14 LAI, J.; COONEY, M. History of photodynamic therapy. **International Ophtamology Clinic**, v. 39, n. 4, p. 163-174, 1999. ISSN 0020-8167.

15 FINSEN, N. R. Remarks on the red-light treatment of small-pox: is the treatment of small-pox patients in broad daylight warrantable? **British Medical Journal,** v. 1, n. 2214, p. 1297-8, June 1903. ISSN 0007-1447 (Print) 0007-1447.

16 TAPPEINER, V. H. Die photodynamische erscheinung (sensibilisierung durch fluoreszierende stoffe). **Ergebnisse der Physiologie,** v. 8, n. 1, p. 698-741, Dec. 1909. ISSN 0080-2042.

17 CIEPLIK, F. *et al*. Antimicrobial photodynamic therapy – what we know and what we don't. **Critical Reviews in Microbiology,** v. 44, n. 5, p. 571-589, Sept. 2018. ISSN 1040-841X.

18 ROBERTSON, C. A.; EVANS, D. H.; ABRAHARNSE, H. Photodynamic therapy (PDT): A short review on cellular mechanisms and cancer research applications for PDT. **Journal of Photochemistry and Photobiology B** - biology**,** v. 96, n. 1, p. 1-8, July 2009. ISSN 1011-1344.

19 KASHEF, N.; HAMBLIN, M. R. Can microbial cells develop resistance to oxidative stress in antimicrobial photodynamic inactivation? **Drug Resistance Updates,** v. 31, p. 31-42, Mar. 2017. ISSN 1368-7646. DOI: 10.1016/j.drup.2017.07.003.

20 LIU, Y. *et al*. Antibacterial photodynamic therapy: overview of a promising approach to fight antibiotic-resistant bacterial infections. **Journal of Clinical and Translational Research,** v. 1, n. 3, p. 140-167, Dec. 2015. ISSN 2382-6533.

21 FONTANA, C. R. *et al*. The antibacterial effect of photodynamic therapy in dental plaque-derived biofilms. **Journal of Periodontal Research,** v. 44, n. 6, p. 751-759, Dec. 2009. ISSN 0022-3484.

22 HAMBLIN, M. R. *et al*. Nanotechnology for photodynamic therapy: a perspective from the laboratory of Dr. Michael R. Hamblin in the Wellman Center for Photomedicine at Massachusetts General Hospital and Harvard Medical School. **Nanotechnology Reviews,** v. 4, n. 4, p. 359-372, Aug. 2015. ISSN 2191-9089.

23 SILVA, A. P. **Novas estratégias para o diagnóstico de onicomicose e tratamento por terapia fotodinâmica**. 2017. 195p. Tese (Doutorado em Ciências). Instituto de Física de São Carlos, Universidade de São Paulo, São Carlos, 2017.

24 BLANCO, K. C. *et al*. Antimicrobial efficacy of curcumin formulations by photodynamic therapy. **Journal of Pharmacy and Pharmacology,** v. 5, n. 8, p. 506-511, 2017. ISSN 2328-2150.

25 FREITAS, M. A. A. *et al*. Bacterial viability after antimicrobial photodynamic therapy with curcumin on multiresistant Staphylococcus aureus. **Future Microbiology,** v. 14, n. 9, p. 739-748, July 2019. ISSN 1746-0913.

26 TONON, C. C. *et al*. Comparative effects of photodynamic therapy mediated by curcumin on standard and clinical isolate of Streptococcus mutans. **Journal of Contemporary Dental Practice,** v. 16, n. 1, p. 1-6, Jan. 2015. ISSN 1526-3711.

27 DOVIGO, L. N. *et al*. Curcumin-mediated photodynamic inactivation of Candida albicans in a murine model of oral candidiasis. **Medical Mycology,** v. 51, n. 3, p. 243-251, Apr. 2013. ISSN 1369-3786.

28 ANDRADE, M. C. *et al*. Effect of different pre-irradiation times on curcumin-mediated photodynamic therapy against planktonic cultures and biofilms of Candida spp. **Archives of Oral Biology,** v. 58, n. 2, p. 200-10, Feb. 2013. ISSN 0003-9969.

29 CORRÊA, T. Q. *et al*. Effects of ultraviolet light and curcumin-mediated photodynamic inactivation on microbiological food safety: a study in meat and fruit. **Photodiagnosis and Photodynamic Therapy,** v. 30, n. 12, p. 101678, June 2020. ISSN 1572-1000.

30 DA SILVA, F. C. *et al*. Fluorescence spectroscopy of Candida albicans biofilms in bone cavities treated with photodynamic therapy using blue LED (450 nm) and curcumin. **Photodiagnosis and Photodynamic Therapy,** v. 26, n. 4, p. 366-370, June 2019. ISSN 1572-1000.

31 DOVIGO, L. N. *et al*. Investigation of the photodynamic effects of curcumin against Candida albicans. **Photochemistry and Photobiology,** v. 87, n. 4, p. 895-903, 2011. ISSN 0031-8655.

32 TORTIK, N. *et al*. A comparative study on the antibacterial photodynamic efficiency of a curcumin derivative and a formulation on a porcine skin model. **Photochemical & Photobiological Sciences,** v. 15, n. 2, p. 187-195, 2016. ISSN 1474-905X.

33 ARAÚJO, N. C. *et al*. Photodynamic antimicrobial therapy of curcumin in biofilms and carious dentine. **Lasers in Medical Sciences,** v. 29, n. 2, p. 629-35, Mar. 2014. ISSN 0268-8921.

34 DA FROTA, M. F. *et al*. Photodynamic therapy in root canals contaminated with Enterococcus faecalis using curcumin as photosensitizer. **Lasers in Medical Sciences,** v. 30, n. 7, p. 1867-72, Sept. 2015. ISSN 0268-8921.

35 PENHA, C. B. *et al*. Photodynamic inactivation of foodborne and food spoilage bacteria by curcumin. **Lwt-Food Science and Technology,** v. 76, Pt. B, p. 198-202, Mar. 2017. ISSN 0023-6438.

36 SOARES, J. M. *et al*. Optimization for microbial incorporation and efficiency of photodynamic therapy using variation on curcumin formulation. **Photodiagnosis and Photodynamic Therapy,** v. 29, p. 101652, Mar. 2020. ISSN 1572-1000. DOI: 10.1016/j.pdpdt.2020.101652.

37 PAOLILLO, F. R. *et al*. The effect of combined curcumin-mediated photodynamic therapy and artificial skin on Staphylococcus aureus-infected wounds in rats. **Lasers in Medical Sciences,** v. 36, n. 6, p. 1219-1226, Aug. 2021. ISSN 0268-8921.

38 SANTOS, D. L. dos *et al*. Curcumin-loaded Pluronic(®) F-127 micelles as a drug delivery system for curcumin-mediated photodynamic therapy for oral application. **Photochemistry & Photobiology Sciences,** v. 97, n. 5, p. 1072-1088, Sept. 2021. ISSN 0031-8655.

39 YIN, R. *et al*. Light based anti-infectives: ultraviolet C irradiation, photodynamic therapy, blue light, and beyond. **Current Opinion in Pharmacology,** v. 13, n. 5, p. 731-62, Oct. 2013. ISSN 1471-4892.

40 NEWMAN, D. J.; CRAGG, G. M. Natural products as sources of new drugs over the nearly four decades from 01/1981 to 09/2019. **Journal of Natural Products,** v. 83, n. 3, p. 770-803, Mar. 2020. ISSN 0163-3864. Available from: https://doi.org/10.1021/acs.jnatprod.9b01285. Accessible at: 14 Mar. 2021.

41 CHEMAT, F.; VIAN, M. A.; CRAVOTTO, G. Green extraction of natural products: concept and principles. **International Journal of Molecular Sciences,** v. 13, n. 7, p. 8615-8627, 2012. ISSN 1422-0067. Available from: https://pubmed.ncbi.nlm.nih.gov/22942724. Accessible at: 14 Mar. 2021.

42 LI, J. W.-H.; VEDERAS, J. C. Drug discovery and natural products: end of an era or an endless frontier?. **Science,** v. 325, n. 5937, p. 161-165, 2009. Available from: https://science.sciencemag.org/content/sci/325/5937/161.full.pdf. Accessible at: 14 Mar. 2021.

43 SUETH-SANTIAGO, V. *et al*. Curcumin, the golden powder from turmeric: insights into chemical and biological activities. **Quimica Nova,** v. 38, n. 4, p. 538-552, May 2015. ISSN 0100-4042.

44 PRIYADARSINI, K. I. The chemistry of curcumin: from extraction to therapeutic agent. **Molecules,** v. 19, n. 12, p. 20091-20112, Dec. 2014. ISSN 1420-3049.

45 PRIYADARSINI, K. I. Photophysics, photochemistry and photobiology of curcumin: Studies from organic solutions, bio-mimetics and living cells. **Journal of Photochemistry and Photobiology C:** photochemistry reviews**,** v. 10, n. 2, p. 81-95, June 2009. ISSN 1389-5567.

46 NELSON, K. M. *et al*. The essential medicinal chemistry of curcumin. **Journal of Medicinal Chemistry,** v. 60, n. 5, p. 1620-1637, Mar. 2017. ISSN 0022-2623.

47 ESATBEYOGLU, T. *et al*. Curcumin: from molecule to biological function. **Angewandte Chemie-International Edition,** v. 51, n. 22, p. 5308-5332, 2012. ISSN 1433-7851.

48 CARMONA-VARGAS, C. *et al*. Combining batch and continuous flow setups in the end-to-end synthesis of naturally occurring curcuminoids. **Reaction Chemistry & Engineering**, v. 2, n. 3, p. 366-374, Aug. 2017.

49 DIAS, L. D. *et al*. Curcumin as a photosensitizer: From molecular structure to recent advances in antimicrobial photodynamic therapy. **Journal of Photochemistry and Photobiology C:** photochemistry reviews**,** v. 45, p. 100384, Dec. 2020. ISSN 1389-5567. DOI: 10.1016/j.jphotochemrev.2020.100384.

50 SOUZA, J. M. *et al*. Impact of continuous flow chemistry in the synthesis of natural products and active pharmaceutical ingredients. **Anais da Academia Brasileira de Ciências,** v. 90, n. 1 Suppl 2, p. 1131-1174, 2018. ISSN 0001-3765.

51 FINLAY, J. C. *et al*. Photobleaching kinetics of Photofrin in vivo and in multicell tumour spheroids indicate two simultaneous bleaching mechanisms. **Physics in Medicine and Biology,** v. 49, n. 21, p. 4837-60, Nov. 2004. ISSN 0031-9155 (Print) 0031-9155.

52 WANG, K. K. *et al*. Explicit dosimetry for photodynamic therapy: macroscopic singlet oxygen modeling. **Journal of Biophotonics,** v. 3, n. 5-6, p. 304-18, June 2010. ISSN 1864-063X (Print) 1864-063x.

53 LIU, B.; FARRELL, T. J.; PATTERSON, M. S. A dynamic model for ALA-PDT of skin: simulation of temporal and spatial distributions of ground-state oxygen, photosensitizer and singlet oxygen. **Physics in Medicine and Biology,** v. 55, n. 19, p. 5913-32, Oct. 7 2010. ISSN 0031-9155.

54 TOVAR, J. S. D. **Study of the principles involved in the activation of indocyanine green by infrared radiation in the photodynamic inactivation of pneumonia**. 2020. Dissertation (Master in Applied Physics) - Instituto de Física de São Carlos, Universidade de São Paulo, São Carlos, 2020.

55 CHIGNELL, C. F. *et al*. Spectral and photochemical properties of curcumin. **Photochemistry and Photobiology,** v. 59, n. 3, p. 295-302, 1994. ISSN 0031-8655.

56 GORMAN, A. A. *et al*. Curcumin-derived transients: a pulsed laser and pulse radiolysis study. **Photochemistry and Photobiology,** v. 59, n. 4, p. 389-398, 1994. ISSN 0031-8655.

57 KHOPDE, S. M. *et al*. Effect of solvent on the excited-state photophysical properties of curcumin. **Photochemistry & Photobiology Sciences,** v. 72, n. 5, p. 625-31, Nov. 2000. ISSN 0031-8655 (Print) 0031-8655.

58 FERNANDEZ, J. M.; BILGIN, M. D.; GROSSWEINER, L. I. Singlet oxygen generation by photodynamic agents. **Journal of Photochemistry and Photobiology B -** biology**,** v. 37, n. 1, p. 131-140, Jan. 1997. ISSN 1011-1344. Available from:

https://www.sciencedirect.com/science/article/pii/S1011134496073496. Accessible at: 09 May 2022.

59 NARDO, L. *et al*. Role of H-bond formation in the photoreactivity of curcumin. **Spectroscopy,** v. 22, p. 928407, 2008. ISSN 2314-4920. Available from: https://doi.org/10.3233/SPE-2008-0335. Accessible at: 02 Mar. 2021.

60 DOS SANTOS, D. P. *et al*. Efficacy of photoactivated Myrciaria cauliflora extract against Staphylococcus aureus infection - a pilot study. **Journal of Photochemistry and Photobiology B -** biology**,** v. 191, p. 107-115, Feb. 2019. ISSN 1011-1344. DOI:10.1016/j.jphotobiol.2018.12.011.

61 HAMBLIN, M. R.; HASAN, T. Photodynamic therapy: a new antimicrobial approach to infectious disease? **Photochemistry and Photobiological Sciences,** v. 3, n. 5, p. 436-50, May 2004. ISSN 1474-905X (Print) 1474-905x.

62 BACELLAR, I. O. *et al*. Photodynamic efficiency: from molecular photochemistry to cell death. **International Journal of Molecular Sciences,** v. 16, n. 9, p. 20523-59, Aug. 2015. ISSN 1422-0067.

63 RIBEIRO, A. P. *et al*. Phototoxic effect of curcumin on methicillin-resistant Staphylococcus aureus and L929 fibroblasts. **Lasers in Medical Science,** v. 28, n. 2, p. 391-8, Feb. 2013. ISSN 0268-8921.

64 LI, L. *et al*. Photodynamic therapy based on organic small molecular fluorescent dyes. **Chinese Chemical Letters,** v. 30, n. 10, p. 1689-1703, Oct. 2019. ISSN 1001-8417.

65 ZHANG, Y. *et al*. A fluorescent photosensitizer with far red/near-infrared aggregation-induced emission for imaging and photodynamic killing of bacteria. **Dyes and Pigments,** v. 165, p. 53-57, June 2019. ISSN 0143-7208. Available from: https://www.sciencedirect.com/science/article/pii/S0143720818324112. Accessible at: 13 July 2022.

66 ALI, Z. *et al*. Determination of curcuminoid content in turmeric using fluorescence spectroscopy. **Spectrochimica Acta Part A:** molecular and biomolecular spectroscopy**,** v. 213, p. 192-198, Apr. 2019. ISSN 1386-1425. DOI: 10.1016/j.saa.2019.01.028.

67 CHEN, X. *et al*. The stability, sustained release and cellular antioxidant activity of curcumin nanoliposomes. **Molecules,** v. 20, n. 8, p. 14293-311, Aug. 2015. ISSN 1420-3049.

68 CHO, J. Y. *et al*. Antifungal activity against Colletotrichum spp. of curcuminoids isolated from Curcuma longa L. rhizomes. **Journal of Microbiology and Biotechnology,** v. 16, n.2, p. 280-285, 2006.

69 HUNG, S. J. *et al*. Efficient photodynamic killing of Gram-positive bacteria by synthetic curcuminoids. **International Journal of Molecular Sciences,** v. 21, n. 23, p. 9024, Nov. 2020. ISSN 1422-0067.

70 HATAMIPOUR, M. *et al*. Demethoxycurcumin: A naturally occurring curcumin analogue for treating non-cancerous diseases. **Journal of Cellular Physiology,** v. 234, n. 11, p. 19320-19330, Nov. 2019. ISSN 0021-9541.

71 XIN, Y. *et al*. Demethoxycurcumin in combination with ultraviolet radiation B induces apoptosis through the mitochondrial pathway and caspase activation in A431 and HaCaT cells. **Tumor Biology,** v. 39, n. 6, p.1-10, June 2017. ISSN 1010-4283.

72 WU, J.; LU, W. Y.; CUI, L. L. Inhibitory effect of curcumin on invasion of skin squamous cell carcinoma A431 cells. **Asian Pacific Journal of Cancer Prevention,** v. 16, n. 7, p. 2813-2818, 2015. ISSN 1513-7368.